

## N O T I C E

THIS DOCUMENT HAS BEEN REPRODUCED FROM  
MICROFICHE. ALTHOUGH IT IS RECOGNIZED THAT  
CERTAIN PORTIONS ARE ILLEGIBLE, IT IS BEING RELEASED  
IN THE INTEREST OF MAKING AVAILABLE AS MUCH  
INFORMATION AS POSSIBLE

**FINAL REPORT FOR**

**NASA Grant NSG-2286**

**WIND TUNNEL SIMULATION OF MARTIAN SAND STORMS**

**(NASA-CR-163262) WIND TUNNEL SIMULATION OF  
MARTIAN SAND STORMS (Santa Clara Univ.)  
31 p HC A03/MF A01 CSCL 03B**

**N80-27257**

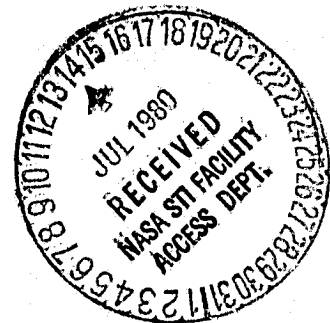
**Unclas  
G3/91 23574**

submitted by

**Ronald Greeley, Principal Investigator  
Department of Physics  
University of Santa Clara  
Santa Clara, CA 95053**

to

**Angelo P. Margozi, Technical Monitor  
Atmospheric Experiments Branch, Mail Stop 245-5  
NASA Ames Research Center  
Moffett Field, CA 94035**



July 8, 1980

## WIND TUNNEL SIMULATION OF MARTIAN SAND STORMS

### Objective

To conduct laboratory simulations of martian windblown processes using the Martian Surface Wind Tunnel at NASA Ames Research Center.

### Background

The Martian Surface Wind Tunnel at NASA Ames Research Center, designed and operated by the Principal Investigator, was utilized to carry out a broad research program to understand the physics and geological relationships of particles driven by the wind under near-martian conditions. This effort was part of a general program of research on aeolian activity as a planetary process funded by the Office of Planetary Geology through the Space Science Division at NASA Ames.

Many physical and chemical processes modify planetary surfaces. On planets having an atmosphere, wind plays an important role in shaping the surface through the redistribution of fine grained material; bedrock may be eroded, and the particles transported for deposition in other areas. This process is readily observable on Earth today, and is evident in the geological record.

Even in its tenuous atmosphere it is now clearly demonstrated that aeolian processes are important on Mars. Mariner 9 results show abundant wind-related landforms including dune fields and yardangs. Viking lander images show drifts of windblown particles; Viking Orbiter pictures add to the inventory of aeolian features. On Venus, measurements made by the Soviet Venera spacecraft show winds that may be capable of transporting

materials and suggest that aeolian processes may operate on that planet as well. In addition, one of the satellites of Saturn, Titan, appears to have an atmosphere and atmospheric surface pressures comparable to Mars, which would again suggest the possibility of aeolian activity.

In order to understand the present surface dynamics and the geological evolution of surfaces for planets subjected to wind, it is important to know the nature of aeolian processes. Factors such as threshold speeds (minimum wind needed to move particles), rates of erosion, trajectories of windblown particles, and flow fields over various landforms are important aspects of the problem.

#### Threshold Experiments

The Martian Surface Wind Tunnel was successfully operated during the grant period to carry out a variety of studies. Rod Leach, assisted by two students from Santa Clara (Mark Plummer and Mary Niemiller) operated the facility. Bruce White and his students from the University of California at Davis were involved with the particle threshold experiments using a carbon dioxide atmosphere. Experimental results were combined with theory by J. Iversen and J. Pollack to account for temperature difference, and a series of curves derived to show minimum wind speeds needed for particle motion to occur on Mars. Results were published in early 1980 (see attached).

#### Erosion Rate Experiments

Preliminary experiments were carried out to determine rates of wind erosion of geological materials. Samples of rocks and minerals were bombarded with grains under simulated windblown conditions under a range of atmospheric pressures and wind speeds following the procedure outlined below:

1. Rock samples were cut 5 mm thick, sized to the MARSWIT Erosion Facility.
2. Slabs were numbered for identification and weighed with a precision balance.
3. Samples were bombarded with various particles, crushed and sized to an average diameter of 160 micrometers. Two types of runs were conducted. Case A runs were at 1 atm. pressure with "Earth air" composition and at "Earth" threshold velocities. Case B runs were at 6 mb pressure, "martian air" composition, and at martian threshold velocities.
4. Samples were then weighed to determine the loss of weight due to erosion, and an erosion rate derived for the two cases.
5. Results were reported at the Lunar and Planetary Science Conference (see attached).

#### Electrostatic Results

Effects of electrostatics on particles in the aeolian environment were studied and a model derived for windblown materials on Mars, published in the Journal of Geophysical Research (see attached).

REPORTS PUBLISHED WHOLLY OR IN PART  
THROUGH THIS GRANT  
(Copies attached)

- Greeley, R. (1979). Silt-clay Aggregates on Mars. J. Geophys. Res., 84, 6248-6254.
- Greeley, R., R. Leach, B. White, J. Iversen and J. Pollack (1980). Threshold Windspeeds for Sand on Mars: Wind Tunnel Simulations. Geophys. Res. Lett., 7, 121-124.
- Greeley, R. and S. Williams (1979). Mars: Preliminary Estimates of Rates of Wind Erosion Based on Laboratory Simulations (abstract). Lunar Planet. Sci. X, 461-463.
- Greeley, R. and R. Leach (1979). "Steam" Injection of Dust on Mars: Laboratory Simulations (abstract). Reports of Planetary Geology Program, 1978-1979, NASA TM-80339, 304-307.
- McKee, T.R., R. Greeley, and D.H. Krinsley (1979). Material Removal and Production of Fines During Aeolian Erosion of Minerals: Mars and Earth. (abstract). Reports of Planetary Geology Program, 1978-1979, NASA TM-80339, 308-310.
- White, B.R., R.N. Leach, J.D. Iversen, and R. Greeley (1979). Calibration of the MARSWIT Tunnel for Determination of Particle Threshold Speeds (abstract). Reports of Planetary Geology Program, 1978-1979, NASA TM-80339, 319-321.
- Williams, S.H. and R. Greeley (1980). Wind Erosion on Mars: An Estimate of the Rate of Abrasion (abstract). Lunar Planet. Sci. XI, 1254-1256.

## SILT-CLAY AGGREGATES ON MARS

Ronald Greeley

Department of Geology and Center for Meteorite Studies, Arizona State University  
 Tempe, Arizona 85281  
 Space Sciences Division, NASA Ames Research Center, Moffett Field, California 95053

ORIGINAL PAGE IS  
 OF POOR QUALITY

**Abstract.** Viking observations suggest abundant silt and clay particles on Mars. It is proposed that some of these particles agglomerate to form sand size aggregates that are redeposited as sandlike features such as drifts and dunes. Although the binding for the aggregates could include salt cementation or other mechanisms, electrostatic bonding is considered to be a primary force holding the aggregates together. Various laboratory experiments conducted since the 19th century, and as reported here for simulated Martian conditions, show that both the magnitude and sign of electrical charges on windblown particles are functions of particle velocity, shape and composition, atmospheric pressure, atmospheric composition, and other factors. Electrical charges have been measured for saltating particles in the wind tunnel and in the field, on the surfaces of sand dunes, and within dust clouds on earth. Similar, and perhaps even greater, charges are proposed to occur on Mars, which could form aggregates of silt and clay size particles. Electrification is proposed to occur within Martian dust clouds, generating silt-clay aggregates which would settle to the surface where they may be deposited in the form of sandlike structures. By analog, silt-clay dunes are known in many parts of the earth where silt-clay aggregates were transported by saltation and deposited as 'sand.' In these structures the binding forces were later destroyed, and the particles reassumed the physical properties of silt and clay, but the sandlike bedding structure within the 'dunes' was preserved. The bedding observed in drifts at the Viking landing site is suggested to result from a similar process involving silt-clay aggregates on Mars.

## Introduction

Aeolian (wind related) processes are recognized as important in modifying the surface of Mars, as evidenced by observations of active dust storms and various erosional and depositional features commonly attributed to wind action. However, after nearly 1 decade of intensive Mars studies, there are still many fundamental questions left unanswered about the aeolian regime of Mars. This report considers the existence of aeolian silt-clay aggregates on Mars and presents a model for their formation.

One of the more intriguing results from the Viking landers is the apparent lack of sand size particles at the two landing sites. The fine-grained material seen on images (Figure 1) is estimated to be considerably less than 100  $\mu\text{m}$  in diameter [H. J. Moore et al., 1977], consistent with estimates of sizes of dust particles in the atmosphere [Pollack et al., 1977]. Yet, observations of bedding structures in the drifts (Figure 1) and of numerous and extensive dune fields on Mars argue for the existence of sand size particles [Cutts and Smith, 1973], because dunes are known to form only from sand size material. Dunes are built from the deposition of saltating particles (and particles in traction), and on earth the particle most commonly transported

by saltation is sand size [Bagnold, 1941]. Although 'sand' is defined as grains about 60-2000  $\mu\text{m}$  in diameter, most dune sand averages 150-300  $\mu\text{m}$  in diameter. This is partly a reflection of the wind speeds needed to initiate movement of grains (threshold wind speeds); as Bagnold [1941] demonstrated, on earth the size most easily moved by the lowest wind speed is about 80  $\mu\text{m}$ . Experiments performed under simulated Martian conditions [Greeley et al., 1976] show that the corresponding grain size for movement by winds on Mars is about 160  $\mu\text{m}$  in diameter. However, this size particle requires an order of magnitude stronger winds, primarily because of the less dense atmosphere on Mars. Therefore one may still expect sand size particles to be the most active grain size moved by wind and to be moved by saltation, but the saltation trajectory would be longer, since the winds would be stronger (as demonstrated by White et al. [1976]). Thus dunes on Mars also should be composed of sand size particles because the basic mechanics of dune formation are the same, even taking into account differences in the Martian environment.

The question of sand on Mars is further complicated by consideration of potential sources. Smalley and Krinsley [1979] point out that most sand on earth is derived from granite, a source that is probably lacking on Mars. It is conceivable that impact cratering of basalts and other rocks on Mars would produce a wide range of fragment sizes, including sand. Sagan et al. [1977], however, have suggested that under the high winds needed to move particles in the Martian atmosphere, the grains would have a short lifetime, leading them to propose the term 'kamikaze' grains. In effect, once the sand is set into motion by the high winds on Mars, the grains would smash into bedrock, other grains, and other objects and be fragmented into tiny (e.g., silt and clay-sized) particles.

On the basis of laboratory experiments, possible terrestrial analogs, and Viking results, a model is proposed in which silt and clay-sized particles agglomerate to form sand size grains on Mars.

## Laboratory Experiments

A series of laboratory experiments was recently undertaken to study rates of aeolian erosion of various rock samples under simulated Martian conditions using both wind tunnel facilities and specially designed apparatus [Greeley and Williams, 1979].

These experiments were designed not only to examine erosion of individual target particles and rock surfaces but also to study effects on the particles doing the abrasion. As Sagan et al. [1977] predicted, sand size particles have very short lifetimes, given the high velocities and nearly 'airless' aeolian environment of Mars. Figure 2 shows experiment results. At a particle velocity slightly above Martian threshold wind speed, sand size material is reduced to particles less than 20  $\mu\text{m}$  in diameter (50% by weight) in about 20 min. Figure 2 also shows, however, that with continued activity the 50% particle size increases after about 60 min. Examination of these particles with a scanning electron microscope (SEM) showed that there



Fig. 1. View from Viking Lander I of the surface of Mars in Chryse Planitia showing drifts of fine-grained windblown deposits. High-resolution images of the drifts show bedding structure, suggesting that the drifts have been partly eroded. Boulder on the left ('Big Joe') is about 1 x 3 m (Viking Lander I image, P-17430).

were many aggregates of fine-grained particles having the overall appearance of miniature popcorn balls (Figure 3). The binding force for the particles was strong enough in some aggregates that they withstood the vibration of a sonic sifter used in sieving to determine the particle size distribution. Further inspection, however, showed that some of the aggregates broke apart during sieving but then re-formed on the smaller screens, suggesting that electrostatic forces were responsible for the agglomeration. Also, when viewed under a scanning electron microscope, the shape of the aggregates would be deformed by the electron beam but still remain as aggregates. The possibility of electrostatic bonding was reinforced when it was observed that the aggregates fell apart when immersed in water where electrostatic forces would be neutralized.

An electrometer was placed on the laboratory apparatus during experiments, and an electrical current of  $2.4 \times 10^{-9}$  to  $2.5 \times 10^{-8}$  A was measured in the impact area. A comparable charge was also observed in wind tunnel simulations [Greeley et al., 1976] for saltating sand grains under simulated Martian conditions. To determine if the results were artifacts due to the experimental apparatus, field measurements of saltating sand were made in the Imperial Valley, California, where an electrical charge of  $1 \times 10^{-9}$  A was measured for a wind speed slightly above threshold. Samples of sand from the field locality were then run in the wind tunnel at 1-bar pressure, and a comparable

charge was measured to the field value. Similar field results have been previously reported by Gill [1948]. The conclusion is thereby drawn that electrostatic charges occur both on wind-blown particles on earth and in simulated Martian conditions and that such charges can hold silt and clay-sized particles together as sand size aggregates.

Considerable research has been conducted on the effects of electrostatics on small particles; see, for example, summaries by Zimon [1969] and A. D. Moore [1973]. Although some consideration has been given to the effects in the Martian environment [Mills, 1977; Eden and Vonnegut, 1973], little attention has been given to their effects related to geological processes. Windblown particles in general may be charged in many ways, including one or more of the following mechanisms: (1) *contact electrification*, resulting from different materials coming into contact or from the contact of the same materials, which have different surface properties, (2) *frictional electrification*, resulting from rubbing one surface over another, (3) *piezoelectric charges*, resulting from pressure, (4) *cleavage*

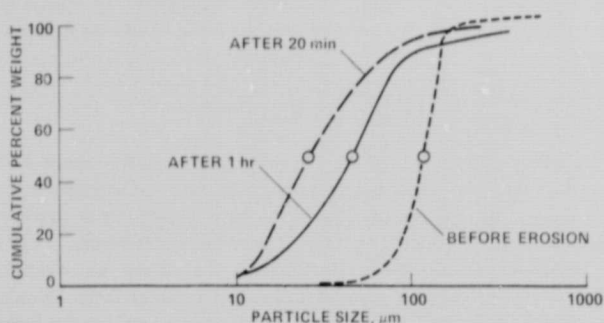


Fig. 2. Size distributions of particles eroded under simulated Martian conditions; velocity of particles was  $61 \text{ m s}^{-1}$ ; atmospheric pressure 5 mbar. Curve on right shows size distribution before experiments; after 20 min of erosion the particle size distribution shifted to a finer size (a reflection of the kamikaze effect of Sagan et al. [1977]); however, as the experiment continued, the size distribution shifted to a larger size as the tiny grains began to accrete (see Figure 3).



Fig. 3. Scanning electron microscope (SEM) photograph of one of larger aggregates from the experiment described in Figure 2; the 'popcorn ball' aggregate is composed of approximately micron size particles held together primarily by electrostatic forces (photograph courtesy of D. K. Krinsley).



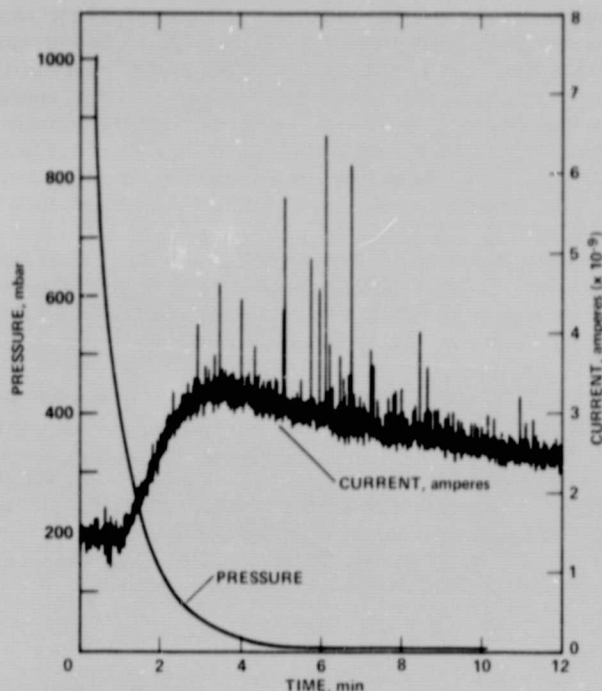


Fig. 4. Current produced by impact of quartz sand ( $\sim 250 \mu\text{m}$  in diameter) as a function of atmospheric pressure; velocity was held constant.

electrification, resulting from breakup of certain minerals [A. D. Moore, 1973], (5) *electrification* resulting from freezing and thawing of water, and (6) *photoelectric charging* [Pinatti and Mascaramas, 1967]. Thus there is ample opportunity for windblown particles to become charged. Electrification may be even more pronounced in the low-density Martian atmosphere than under conditions on earth. Paschen's curve shows spark breakdown voltage [Cobine, 1941; Llewellyn-Jones, 1957] as a function of atmospheric pressure for  $\text{CO}_2$  and earth air. Although the exact value for electrical breakdown depends upon a number of factors, the curves illustrate that the minimum values are reached at pressures in the range for the surface of Mars. Thus on Mars the atmosphere becomes conducting at very low electrical potentials compared to earth.

Laboratory experiments were conducted to address the question of how electrification of particles could occur under Martian conditions and what the effects would be on aeolian processes. Three factors were studied: (1) the effect of reduced atmospheric pressure, (2) the effect of high particle velocities associated with strong winds needed to move particles on Mars, and (3) the effect of particle size on charge. Figure 4 shows the electrical current produced by impact of windblown quartz sand 175-355  $\mu\text{m}$  in diameter on a planar copper plate for a range of atmospheric pressures. As pressure is reduced from 1 atm to 4 mbar, the current produced is first quadrupled—but is very irregular with many 'spikes'—and then settles at a value  $1\frac{1}{2}$  times greater than at 1 atm. The high initial current is thought to result from the fracturing of the grains due to more violent collisions which take place between particles when cushioning effects of the denser air are reduced at lower pressure. Initially, the more easily fractured particles were broken, generating cleavage electrification. As the test continued, frequency of the high current spikes decreased, and only the more stable grains remained. During aeolian activity on Mars, this would result in higher electrification than on earth, possibly with relatively high charges produced in the initial stages of wind storms.

Experiments were also conducted to determine the effect of velocity on electrification. Figure 5 shows that with increasing particle velocity there is a corresponding increase in current, again probably resulting from increased energetic collisions that resulted in greater 'cleavage' (and fracturing) electrification. A reversal in electrical sign from positive to negative at the higher velocities also occurred.

Changes in electrical sign within the same material were also observed as a function of particle size. Figure 6 shows current as a function of particle size (velocity and pressure held constant) for several materials. Depending upon the material, the sign changed with particle diameter.

The conclusion drawn from review of the effects of electrostatics of particles and from laboratory experiments carried out under simulated Martian environments is that (1) electrification of windblown particles occurs on earth, (2) under Martian conditions, electrification is enhanced because of reduced atmospheric pressure and the high velocities required for wind

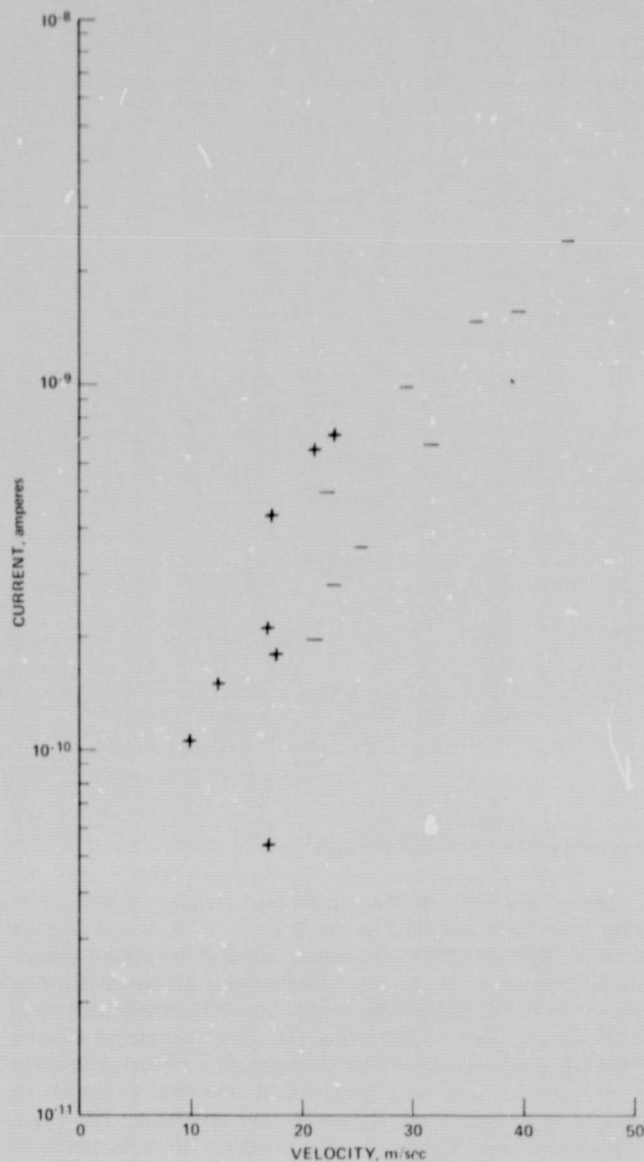


Fig. 5. Current produced by the impact of quartz sand ( $\sim 120 \mu\text{m}$  in diameter) as a function of impact velocity; note that there is a change in sign from positive to negative at the higher velocities.

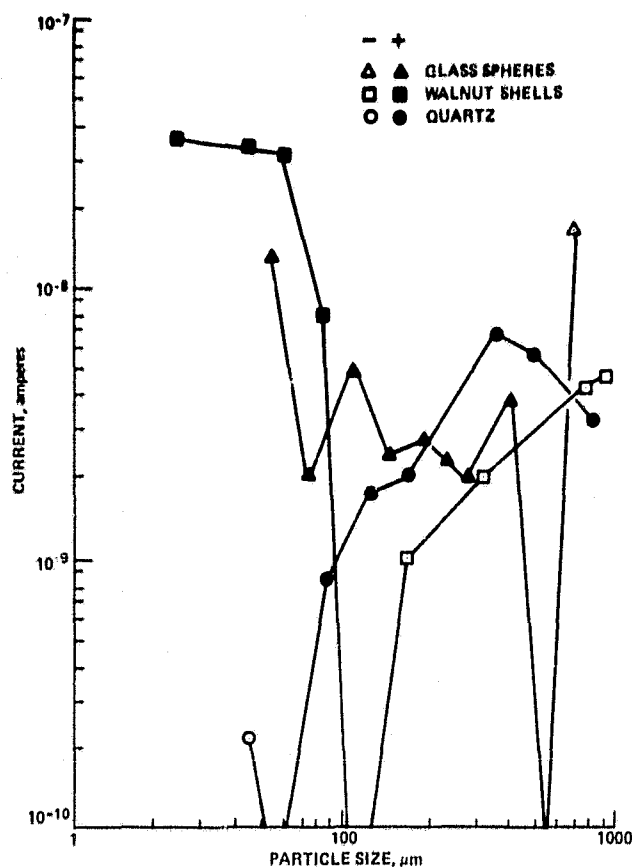


Fig. 6. Current produced by impact of particles of different composition as a function of particle size; note that not only is there an effect of composition and size on current but that the electrical sign changes as well.

transport, and (3) the current produced and electrical sign of individual particles within a cloud of windblown particles are functions of wind velocity (and hence particle velocity), particle composition, and particle size. The aggregates described in the first part of this section can be explained as being held together primarily by electrostatic forces, and similar aggregates not only may be expected to form on Mars, but their formation is probably enhanced. Although such aggregates may be relatively weak, they are proposed to explain the formation of some sandlike structures on Mars, as will be described later. First, however, consideration will be given to possible analogs on earth.

#### Silt-Clay Dunes on Earth

Dunes and other aeolian deposits composed of silt and/or clay have been described in many parts of the world (Bowler [1973], Butler [1974], and others). One of the earliest reports of clay dunes is by Coffey [1909], who described dunelike ridges many kilometers long, more than 100 m wide, and 10 m high on the Texas Gulf Coast. He observed grains of sand blowing across the ridges; closer inspection indicated that the sand particles were clay pellets that crumbled between the fingers but which were strong enough to saltate. The Texas clay dunes were studied in more detail by Huffman and Price [1949] and, as Coffey had proposed earlier, were found to result from a combination of location (proximity to coastal brackish lagoons) and climate (dry). Clay crusts were found to develop on the dried lagoons where salts had crystallized

within the silt and clay and acted as a cement; as the crusts cracked and curled, sharp edges were exposed to the wind. Winds blowing across the dried surface eroded pieces of the crust, which, during transport, developed into the sandlike 'pellets' described by Coffey. The pellets behaved essentially as sand as long as they remained dry and were deposited in the form of dunes. When wetted, however, the binding forces for the pellets were destroyed, and the clay dunes became stabilized.

Similar modes of formation of silt-clay dunes have been described in the Colorado Desert [Roth, 1960]; Figure 7 shows a silt-clay dune at Clark Dry Lake, California, in which the bedding and other internal structures are essentially the same as 'normal' sand dunes. Thus even though wetting stabilizes silt-clay dunes, the internal structure is preserved. Although the process of agglomeration involves primarily cementation, and electrostatic bonding of aggregates has not been reported on earth (it probably has not been sought), the important point is that both the external morphology and internal bedding structures of dunes and other sandlike forms can result from silt and clay aggregates under certain conditions.

#### The Mars Model

It is proposed that *some* of the dunes, drifts, and other sandlike features on Mars are composed of sand size aggregates of silt and clay particles that are held together by electrostatic forces and/or salt cementation, at least during the transportation and deposition phases. Several different mechanisms for the formation of the aggregates may occur on Mars.

#### Derivation From Surface Deposits

Consideration of the mechanical properties of the fine material at both landing sites [H. J. Moore et al., 1977] indicates that it is cohesive and is probably composed of silt and clay. The term *duricrust* has been applied to the upper layer of these deposits. The binding agent for duricrust could be electrostatic, salt cements (salt weathering on Mars has been discussed by Malin [1974]), or other interparticle forces. When the duricrust is disturbed—as, for example, by small mass movements [Binder et al., 1977]—it displays irregular edges that would be susceptible to wind erosion and the formation of silt-clay pellets similar to those described by Coffey [1909] for the Texas Gulf Coast. Although it may be argued that the pellets would be destroyed rapidly under the high winds needed for particle threshold on Mars, several opposing factors may operate. First, threshold wind speeds needed to move the pellets would be lower than for comparable sizes for 'real' sand because, as aggregates, the pellets would be less dense [Greeley et al., 1974a, 1977]. In addition, because the pellets would be derived from the edges of duricrust or from other aerodynamically 'sharp' places, lower wind velocities could set them into motion than could if they were present on flat beds. Thus lower wind velocities would be necessary for pellet movement than for real sand, and if the binding strength were high enough, the pellets could survive saltation; measurements of the strength, however, have not been made.

A second consideration involves the cascading effect. As Bagnold [1941] demonstrated, dynamic threshold speeds involving initiation of particle motion through impact by material already in motion is considerably lower than static threshold speeds. Thus even though the pellets may smash upon impact, they could impart enough energy to set other material into the airstream which would generate a cascade of material

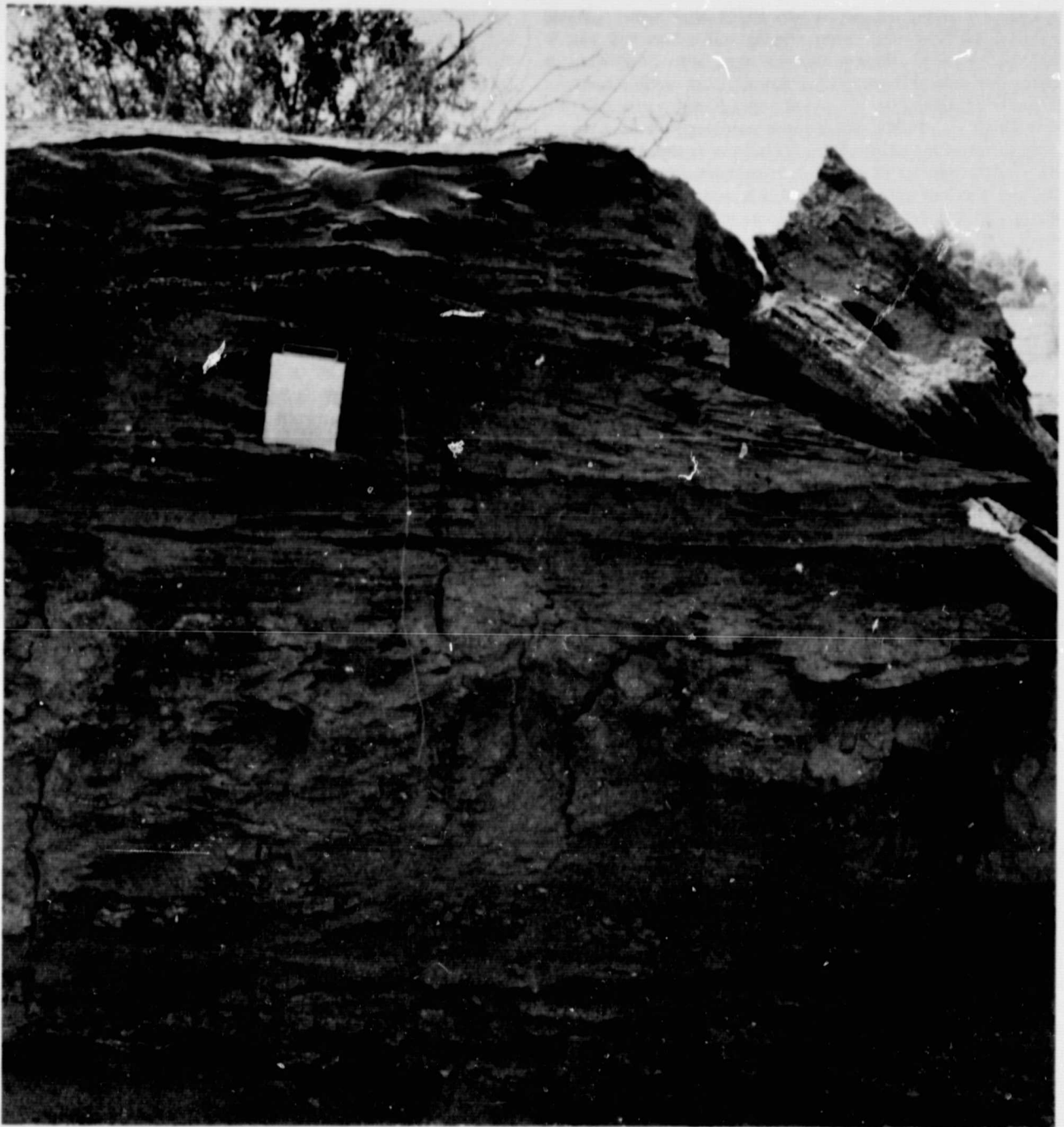


Fig. 7. Exposed section of a silt-clay dune in Clark Dry Lake, California, showing bedding structure similar to sand dunes. Metal plate is about 7 cm long and indicates scale (photograph by Ron Papson, 1977).

moving under relatively low wind speeds. Some of the silt and clay derived from the smashed pellets would probably go into suspension as a dust cloud.

#### Pellet Accretion During Dust Storm Settling

Aggregates of sand size pellets may form from the fine, micron size particles that occur in dust storms. Contact and frictional electrification of the grains could be expected within the dust clouds; given differences in composition, particle size, and collisional velocity within the cloud, both positive and negative charges would occur. As the dust storm progresses, the charges may be cumulative until sufficient charges are reached

when aggregation begins. Once they begin to form, the aggregates would settle out of the cloud much more quickly than the settling rates of the individual dust grains. Formation of the aggregates may be an effective mechanism for ending the dust storms on Mars. As an analog it is well established that dust storms on earth are highly electrified [Boning, 1927; Kamra, 1972], and it has been proposed [Beavers, 1957] that aggregates of clay minerals were electrostatically attracted and deposited as loess in the geological past. It is not known, however, how large the aggregates might grow.

For the Martian case, as the aggregates settle toward the surface, they could be placed into saltation by local winds, or gusts, behaving as sand, and be deposited in drifts, dunes, etc.

It has been noted [Sagan et al., 1972] that some 'variable features' such as dark crater streaks and other dark albedo patterns begin to develop and are most active following or during the waning stages of dust storms. Dark crater streaks are generally considered to be eroded zones [Greeley et al., 1974b; Veverka et al., 1974] where loose particles have been swept away to reveal a darker substrate. Dark crater streaks have been observed to expand in areal extent to many square kilometers on time scales of only weeks, and it is assumed that the wind-blown particles eroded are of the size most readily moved, or about 160  $\mu\text{m}$  in diameter. Thus one sequence might be that aggregates of sand size grains settle from dust clouds as a thin mantle of loose particles; local gusts and turbulence around craters and other landforms sweep away the aggregates while they are still loosely bonded. With time, in the highly conductive Martian atmosphere, the charges bonding the aggregate would 'leak' away, and the particles would reassume the physical properties of individual particles of silt and clay.

#### Accretion During Saltation

Accretion of pellets may also occur within a saltation cloud. Once wind speeds are sufficiently strong to set either real sand or existing aggregates into motion, then the cascading effect described above may set other material into motion, including fine (silt and clay) particles. Once entrained by the wind, electrification could occur within the cloud, which could lead to accretion. Even though pellets may be destroyed on impact with the surface, or from interparticle collisions within the cloud, aggregates may be constantly reforming in a manner similar to that observed during sieving of the laboratory samples. The mass of the windblown material, however, could behave as sand, forming sandlike structures such as dunes.

#### Discussion

If aggregates of silt and clay form on Mars into sand size pellets that are cohesive enough for transport, then several interesting effects may occur. First, their formation could explain the apparent contradiction between observations at the landing sites showing no sand size particles and the observations of drifts with internal bedding indicative of sand. In addition, some dunes seen from orbit could consist of aggregates. The mechanism could also explain the relative stability of the light streaks in comparison to dark streaks. Light streaks are generally considered to be aeolian deposits, whereas most dark streaks are thought to be eroded zones [Greeley et al., 1974b]. Light streaks remain relatively fixed and inactive for years, whereas the dark zones shift on time scales of only weeks. The white streaks could be deposits of silt and clay that were emplaced as aggregates, or pellets that were sand size—hence relatively easily moved by the wind. After their emplacement, however, the binding forces may have been lost (as the case of the clay dunes described by Coffey [1909] and Huffman and Price [1949], and the pellets would disaggregate *in situ*. The deposit would then reassume its physical properties as silt and clay and be very difficult to erode. If the binding force were electrostatic, then in the highly conductive Martian environment, the charge could be expected to 'leak' away within short time scales. Moreover, the high albedo of the light streaks is consistent with fine-grained material such as silt or clay.

In addition, aggregates may account for the lower rates of erosion on Mars than had been anticipated prior to Viking. The high frequency of dust storms observed for many years and the high wind speeds needed to move particles led many investi-

gators (Sagan [1973] and others) to predict very high rates of aeolian erosion on Mars. Viking results, however, indicate relatively low rates of erosion [Arvidson et al., 1979]. The low rates could be accounted for if many of the saltating grains are aggregates, because they would not be very effective agents of erosion in comparison to whole grains.

The model proposal here is not considered to apply to all Martian aeolian features. Undoubtedly, many of the sand dunes observed do involve 'true' sand particles, not aggregates. The mechanism proposed, however, may account for some of the observations of the Martian aeolian features.

*Acknowledgements.* Gratitude is expressed to Rodman Leach for carrying out experiments dealing with electrostatics. David Krinsley is thanked for SEM photographs of the silt-clay aggregates used herein. Helpful comments on the manuscript were provided by D. Krinsley, R. Leach, A. Peterfreund, S. Williams, and A. A. Mills. This work was carried out under grant NSG-2284 to Arizona State University and grant NSG-2286 to the University of Santa Clara, both from the Office of Planetary Geology, National Aeronautics and Space Administration.

#### References

- Arvidson, R., F. Guinness, and S. Lee, Differential aeolian redistribution rates on Mars, *Nature*, 278, 533-535, 1979.
- Bagnold, R. A., *The Physics of Blown Sand and Desert Dunes*, 265 pp., Methuen, London, 1941.
- Beavers, A. H., Source and deposition of clay minerals in Peonian loess, *Science*, 126(3286), 1285, 1957.
- Binder, A. B., R. E. Arvidson, E. A. Guinness, K. L. Jones, E. C. Morris, T. A. Mutch, D. C. Pieri, and C. Sagan, The geology of the Viking Lander 1 site, *J. Geophys. Res.*, 82, 4439-4451, 1977.
- Boning, P., Dust electricity, *Z. Tech. Phys.*, 8, 385, 1927.
- Bowler, J. M., Clay dunes: Their occurrence, formation and environmental significance, *Earth Sci. Rev.*, 9, 315-338, 1973.
- Butler, B. E., A contribution towards the better specification of parna and some other aeolian clays in Australia, *Z. Geomorphol.*, 20, 106-116, 1974.
- Cobine, J. D., *Gaseous Conductors*, McGraw-Hill, New York, 1941.
- Coffey, G. N., Clay dunes, *J. Geol.*, 17, 754-755, 1909.
- Cutts, J. A., and R. S. U. Smith, Eolian deposits and dunes on Mars, *J. Geophys. Res.*, 78, 4139-4154, 1973.
- Eden, H. F., and B. Vonnegut, Electrical breakdown caused by dust motion in low-pressure atmospheres: Consideration for Mars, *Science*, 180, 962-963, 1973.
- Gill, E. W. B., Frictional electrification of sand, *Nature*, 162, 568, 1948.
- Greeley, R., and S. Williams, Mars: Preliminary estimates of rates of wind erosion based on laboratory simulations, *Lunar Planet. Sci.*, 10, 461-463, 1979.
- Greeley, R., J. D. Iversen, J. B. Pollack, N. Udovich, and B. White, Wind tunnel studies of martian aeolian processes, *Proc. Roy. Soc., Ser. A*, 341, 331-360, 1974a.
- Greeley, R., J. D. Iversen, J. B. Pollack, N. Udovich, and B. White, Wind tunnel simulations of light and dark streaks on Mars, *Science*, 183, 847-849, 1974b.
- Greeley, R., B. White, R. Leach, J. Iversen, and J. Pollack, Mars: Wind friction speeds for particle movement, *Geophys. Res. Lett.*, 3, 417-420, 1976.
- Greeley, R., B. R. White, J. B. Pollack, J. D. Iversen, R. N. Leach, Dust storms on Mars: Considerations and simulations, *NASA Tech. Memo.*, TM 78423, 29 pp., 1977.

- Huffman, G. G., and W. A. Price, Clay stone formation near Corpus Christi, Texas, *J. Sediment. Petrology*, **19**, 118-127, 1949.
- Hewellyn Jones, F., *Ionization and Breakdown in Gases*, John Wiley, New York, 1957.
- Kamra, A. K., Measurements of the electrical properties of dust storms, *J. Geophys. Res.*, **77**, 5885a-5869, 1972.
- Mahn, M. C., Salt weathering on Mars, *J. Geophys. Res.*, **79**, 3888-3894, 1974.
- Mills, A. A., Dust clouds and frictional generation of glow discharges on Mars, *Nature*, **268**, 614, 1977.
- Moore, A. D., *Electrostatics and Its Application*, p. 84, John Wiley, New York, 1973.
- Moore, H. J., R. E. Hutton, R. F. Scott, C. R. Spitzer, and R. W. Shorthill, Surface materials of the Viking Lander sites, *J. Geophys. Res.*, **82**, 4497-4523, 1977.
- Pinatti, D., and S. Mascarenhas, Electrical currents produced during the solidification of water, *J. Appl. Phys.*, **38**, 2648-2652, 1967.
- Pollaek, J. B., D. Colburn, R. Kahn, J. Hunter, W. Van Camp, C. E. Carlston, and M. R. Wolf, Properties of aerosols in the Martian atmosphere, as inferred from Viking Lander data, *J. Geophys. Res.*, **82**, 4479-4496, 1977.
- Roth, F. S., The silt-clay dunes at Clark Dry Lake, California, *Compass*, **38**, 18-27, 1960.
- Sagan, C., Sandstorms andolian erosion on Mars, *J. Geophys. Res.*, **78**, 4155-4161, 1973.
- Sagan, C., J. Veverka, P. Fox, R. Dubisch, J. Lederberg, I. Eximihal, I. Quam, R. Tucker, J. B. Pollack, and B. A. Smith, Variable features on Mars. Preliminary Mariner 9 television results, *Icarus*, **17**, 346-372, 1972.
- Sagan, C., D. Pierz, P. Fox, R. E. Arvidson, and E. A. Guinness, Particle motion on Mars inferred from the Viking Lander cameras, *J. Geophys. Res.*, **82**, 4430-4438, 1977.
- Smalley, I. J., and D. H. Kinsley, Aeolian sedimentation on Earth and Mars. Some comparisons, submitted to *Icarus*, 1979.
- Veverka, J., C. Sagan, I. Quam, R. Tucker, and B. Fross, Variable features on Mars. III. Comparison of Mariner 1969 and Mariner 1971 photography, *Icarus*, **21**, 319-368, 1974.
- White, B. R., R. Greeley, J. D. Iversen, and J. B. Pollack, Estimated grain saltation in a Martian atmosphere, *J. Geophys. Res.*, **81**, 5643-5650, 1976.
- Zimon, A. D., *Adhesion of Dust and Powder*, translated from Russian by M. Corn, Plenum, New York, 1969.

(Received February 6, 1979  
 revised April 5, 1979  
 accepted April 9, 1979.)

THRESHOLD WINDSPEEDS FOR SAND ON MARS WIND TUNNEL SIMULATIONS

R. Greeley

Center for Meteorite Studies, Arizona State University  
Tempe, Arizona 85281

R. Leach

University of Santa Clara and NASA-Ames Research Center  
Moffett Field, California 94035

B. White

Department of Mechanical Engineering, University of California at Davis  
Davis, California 95616

J. Iversen

Department of Aerospace Engineering, Iowa State University  
Ames, Iowa 50011

J. Pollack

Space Sciences Division, NASA-Ames Research Center  
Moffett Field, California 94035

PRECEDING PAGE BLANK NOT FILMED

**Abstract.** Wind friction threshold speeds ( $u_{*t}$ ) for particle movement (saltation) were determined in a wind tunnel operating at martian surface pressure with a 95 percent  $\text{CO}_2$  and 5 percent air atmosphere. The relationship between friction speed ( $u_*$ ) and free-stream velocity ( $u_\infty$ ) is extended to the critical case for Mars of momentum thickness Reynolds numbers ( $Re_\theta$ ) between 425 and 2000. It is determined that the dynamic pressure  $\rho u_\infty^2$  required to initiate saltation is nearly constant for pressures between 1 bar (Earth) and 4 mb (Mars) for atmospheres of both air and  $\text{CO}_2$ ; however, the threshold friction speed ( $u_{*t}$ ) is about 10 times higher at low pressures than on Earth. For example, the  $u_{*t}$  (Earth) for particles 210  $\mu\text{m}$  in diameter is  $0.22 \text{ m s}^{-1}$  and the  $u_{*t}$  (Mars, 5 mb, 200 K) is  $2.2 \text{ m s}^{-1}$ .

by Greeley *et al.* (1976, 1977) were run not in an atmosphere of martian composition (primarily  $\text{CO}_2$ ), but rather in 'Earth' air. Extrapolations were made to the martian atmospheric composition by taking into account the differences in molecular weight between  $\text{CO}_2$  and 'Earth' air. However, because the dynamics of  $\text{CO}_2$  at low pressures and at the relatively low Reynolds numbers involved with the martian aeolian environment are so poorly understood, these extrapolations were open to question. Consequently, MARSWIT was modified to enable experiments to be run in a 95 percent  $\text{CO}_2$  atmosphere. The experiments described earlier (Greeley *et al.*, 1976) were duplicated in the  $\text{CO}_2$  atmosphere to generate a set of threshold curves for particle motion on Mars. The results of these experiments are the subject of this report.

Introduction

A great deal of attention has been given to the problem of wind-blown particles on Mars, beginning with a paper by Sagan and Pollack (1969). Most investigations have involved estimations of wind speeds needed to initiate movement of particles of different sizes and densities based on the work originally done by Bagnold (1941) who described the physics for windblown sand on Earth. Extrapolations were made to Mars by substituting the appropriate parameter values for Mars in the equations derived by Bagnold for Earth (Sagan and Pollack, 1969; Arvidson, 1972; Iversen *et al.*, 1973, and others). Some studies (Chang *et al.*, 1968; Adlon *et al.*, 1969) incorporated into the extrapolations data from laboratory simulations of some of the conditions on Mars. An extrapolation taking interparticle force into account, more appropriate for martian pressures, was obtained by Iversen *et al.* (1976).

To provide better simulations, an open circuit wind tunnel (Martian Surface Wind Tunnel or MARSWIT) was constructed at NASA-Ames Research Center (the facility is described in Greeley *et al.*, 1977). Experiments from MARSWIT yielded estimates of wind friction speeds for particle movement on Mars in which nearly all the important parameters were physically simulated or otherwise taken into account. Two of the most important parameters for martian simulations are gravity and the atmospheric conditions at the surface. For simulations of Mars on Earth the primary effect of gravity may be accounted for partly by using proportionately lower density particles than those expected on Mars. The atmosphere is more difficult to simulate. Although MARSWIT is capable of operating down to about 3 mb pressure, the experiments presented

Experimental Procedure and Results

The test procedure was as follows: A bed of uniform-sized particles was placed in the wind tunnel test section and the surface was smoothed. For each test a 2.5 meter long bed of material was used, as previous tests showed (Greeley *et al.*, 1977) that a bed of this length would give very nearly the same results as an infinitely long bed whereas shorter beds resulted in increased saltation threshold values. The tunnel was located inside a large vacuum chamber which was evacuated to about 4 mb pressure using 'Earth' air. The tunnel was then started and the wind speed gradually increased until saltation threshold was reached. The tunnel was stopped and started several times at each test condition to obtain a number of data points. Three separate methods were used to determine saltation threshold: (1) A high resolution closed-circuit television system was used to observe the particle movement directly; (2) a laser-photocell system indicated saltation by the attenuation of the signal due to particles interrupting the laser beam; and (3) an electrostatic detector measured the current produced by saltating particles impinging on the detector element. For most experiments all the systems were used concurrently to detect saltation, with the electrostatic system being more sensitive for small particles and the television and laser systems more sensitive for the larger particles. Many materials were tested but ground walnut shells (specific gravity 1.1) were deemed to best represent martian particles (Greeley *et al.*, 1977) and were used to generate the data presented here.

The chamber was then filled with  $\text{CO}_2$  to a pressure of about 80 mb giving a 95 percent  $\text{CO}_2$  and 5 percent air mixture. Threshold tests were run at various pressures as the chamber pressure was again reduced to 4 mb. Finally, the chamber was purged with air and pumped to 4 mb for the third series of tests. Threshold speeds were again taken with air as the working

Copyright 1980 by the American Geophysical Union.

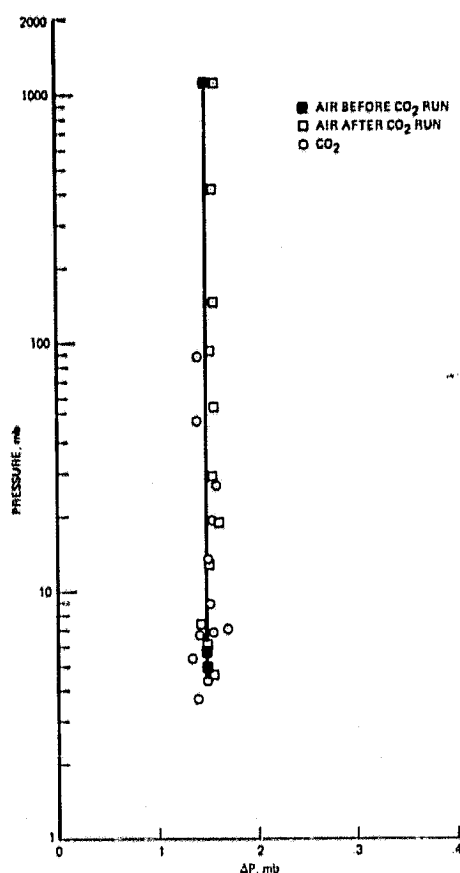


Figure 1. Dynamic pressure at the wind tunnel centerline to initiate particle saltation with 5 percent air and 95 percent  $\text{CO}_2$  mixture for ground walnut shell particles  $212 \mu\text{m}$  in diameter.

fluid, as the chamber was step-filled to atmospheric pressure to obtain threshold speeds for a range of pressures. With this technique it was possible to compare a particular bed of material with all conditions nearly identical except that the working fluid was changed from air to  $\text{CO}_2$  and back to air. By comparing the initial air data with the final air data a good estimation of the repeatability of the data could be made. Figures 1 and 2 present typical data sets for a single test bed. Note that the dynamic pressure ( $\Delta p$ ) is nearly constant for both air and 95 percent  $\text{CO}_2$  and with chamber pressure (Fig. 1); the velocities (Fig. 2) are different due to the differences in properties of air and  $\text{CO}_2$ . This procedure was followed for each particle size tested over the range of diameters from  $23 \mu\text{m}$  to  $800 \mu\text{m}$ .

#### Data Reduction

The critical measurements in the wind tunnel are the differential pressure ( $\Delta p$ ) between the total pressure ( $p_t$ ) and the static pressure ( $p_s$ ) at the tunnel centerline, and the chamber pressure and temperature. The tunnel centerline wind velocities can then be calculated from these measurements, as well as the friction velocity ( $u_*$ ) for a given bed of materials taking into account the boundary layer profile and the surface roughness, as discussed in Iversen *et al.* (1973, 1976).

Time-averaged boundary layer velocity profiles were determined from differential pressure measurements between static pressure and a total head pressure tube that was transversed through the boundary layer. The tests showed the boundary flow to be essentially steady, two-dimensional, constant-property (i.e., maintaining a constant chamber pressure), and to have a constant free-stream velocity turbulent flow through the tunnel. A zero-pressure-gradient flow was achieved by increasing the top tunnel wall height with increasing downstream distance (thereby expanding the cross sectional area); the zero-pressure-gradient was verified

by static pressure measurements at several positions in the tunnel. A naturally turbulent boundary layer developed for most of the flow conditions; however, at the lower pressures it was necessary to "trip" the boundary layer by placing small pebbles on the tunnel floor in the entrance section of the tunnel. The test section was more than 25 boundary-layer thickness-lengths from the pebbles placed upstream, insuring a fully developed turbulent core region at low pressures.

The data were reduced taking into account Mach number and slip flow effects in the velocity determination. Each profile was numerically curve fitted by means of a multi-piecewise cubic spline technique.

For the turbulent boundary layer the value of the friction speed  $u_*$  is dependent on the value of the momentum thickness Reynolds Number

$$Re_{\theta} = \frac{u_{\infty} \theta}{\nu} \quad (1)$$

where  $u_{\infty}$  is the free-stream wind-tunnel speed,  $\nu$  is the kinematic viscosity, and  $\theta$  is the momentum-deficit thickness. The momentum-deficit thickness is defined as the thickness of the layer as measured from the wall of an external stream (at constant speed  $u_{\infty}$ ) containing a momentum flux equal to the loss of momentum flux due to the presence of the wall. It is convenient to define the momentum-deficit thickness  $\theta$  in terms of mean velocity profiles as

$$\theta = \int_0^{\delta} \frac{u}{u_{\infty}} \left( 1 - \frac{u}{u_{\infty}} \right) dy \quad (2)$$

where  $\delta$  is the boundary layer height at which the value of velocity  $u$  is 99 percent that of  $u_{\infty}$ , and  $y$  is the vertical height. The momentum thicknesses were determined from integrating the resultant curve fit by a numerical quadrature technique.

An analysis of the zero-pressure-gradient turbulent boundary layer for low Reynolds numbers has been made by Coles (1962); from this work the surface shear stress  $\tau_0$  can be determined from the velocity profiles obtained in the wind tunnel. This is accomplished by assuming that the velocity obeys the logarithmic law

$$\frac{u}{u_*} = \frac{1}{\kappa} \ln \frac{u_* y}{\nu} + C \quad (3)$$

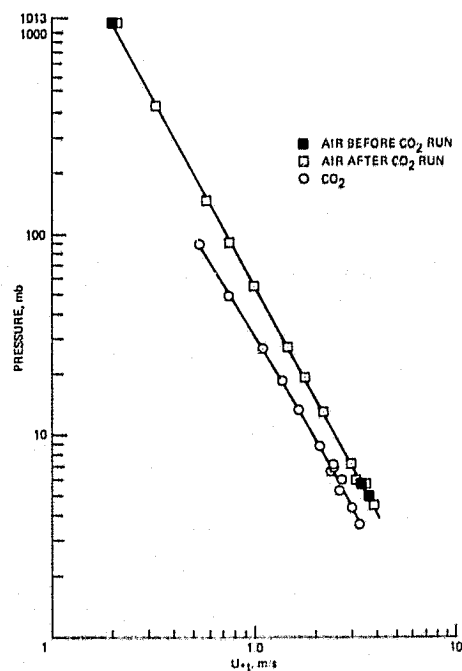


Figure 2. Wind tunnel centerline velocity to initiate particle saltation threshold with air and 95 percent  $\text{CO}_2$ -air mixture for ground walnut shells  $212 \mu\text{m}$  in diameter.

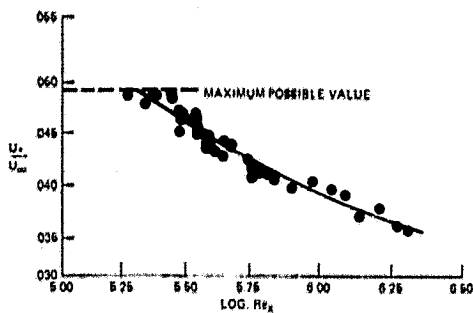


Figure 3. The ratio of friction velocity ( $u_*$ ) to wind tunnel centerline velocity ( $u_\infty$ ) as determined by boundary layer surveys and presented as a function of Reynolds number ( $Re_x$ ) based on the distance from the beginning of the wind tunnel to the test point.

for the wall region ( $y < 0.2$ ) excluding the viscous sublayer. In this study,  $\kappa = 0.418$  and  $C = 5.45$ , as determined by Patel (1965). Converting to  $\log_{10}$  gives

$$\frac{u}{u_*} = 5.5 \log_{10} \frac{u_* y}{\nu} + 5.45 \quad (4)$$

The ratio  $u_*/u_\infty$  is well fit by the empirical equation ( $600 > Re_\theta > 2000$ )

$$\frac{u_*}{u_\infty} = 0.702 (\log_{10} Re_x)^{-1.59} \quad (5)$$

as shown by Figure 3. In this equation the relationship is presented as a function of  $Re_x$ , the Reynolds number based on the distance from the beginning of the wind tunnel to the test point. For flows with lower values of  $Re_\theta$  ( $Re_\theta < 600$ ) the ratio  $u_*/u_\infty$  becomes a constant value of approximately 0.049. This is the maximum value that  $u_*/u_\infty$  can obtain in a turbulent boundary layer at low Reynolds numbers (White, 1979 and Barr, 1979). For values of  $Re_\theta$  less than 425 the boundary layer flow is laminar and is of no importance in flows of saltating particles.

Using these relationships the data are presented as a function of particle size versus friction threshold velocity for various pressures (Fig. 4). These data are valid for particles larger than about  $60 \mu\text{m}$ , but some adjustment upward may be necessary for the smaller particles as indicated by the following analysis:

Tests were conducted to determine if the angle of repose, which is a function of various interparticle forces, was affected by reducing the ambient pressure. Results show that smaller sized particles are affected; for example, particles  $20 \mu\text{m}$  in diameter have a much lower angle of repose at 4 mb than at 1 bar, if the tests were run immediately upon reaching the lower pressure. If, however, the particles were allowed to remain at the lower pressure for 24 hours before the test was made, the angle of repose was the same at 1 bar. Evidently, interparticle air acts as a lubricant as it escapes, causing the particles to flow over one another more readily in a low-pressure environment. If allowed to remain at low pressure for a period of time (many hours), the interparticle air slowly outgasses and no longer affects the angle of repose. Ideally, the smaller test particles should be allowed to stabilize in the evacuated wind tunnel for a sufficient period of time for all interparticle gas to escape before saltation threshold tests commence. This, however, was not possible within the limitations of MARSWIT. Thus, the data for the particles less than  $60 \mu\text{m}$  show lower thresholds than if the material had been held at low pressure long enough for all interparticle gas to escape. (For an analysis of the relationship between angle of repose and the threshold velocity see Bagnold, 1941, Chapter 7.) Because of this effect the two smaller sizes of particles tested showed a decrease in dynamic pressure required for saltation with decreasing chamber pressure in contrast to the larger sizes tested. This decrease is attributed to the lubricating effect of the escaping interparticle gas, and correcting for this effect by assuming a constant  $\Delta p$ , the final data curve Figure 5 is presented as the best experimental determination of threshold friction velocity  $u_{*t}$  for particles on Mars. These data are also adjusted for

representative martian temperatures by the method presented by Iversen et al. (1976).

The particle threshold curves presented here indicate that somewhat lower wind speeds are required to move particles on Mars than had been predicted by earlier studies. This is due primarily to a more refined method of determining the relationship between free stream velocity and friction velocity as well as a better simulation using  $\text{CO}_2$  as the working fluid.

#### Discussion and Comparison with Conditions at the Viking Lander Sites

We have used the results to make a preliminary assessment of the ability of winds to move sand sized particles at the Viking Lander Sites. To do this, we first relate friction velocity to winds measured by the lander meteorology experiment at a height of 1.6 m above the surface and winds at the top of the planetary boundary layer. Both lander sites are characterized by fairly flat terrain covered with fine grained material, but littered with numerous rocks (Mutch et al., 1976a, b). A reasonable choice for the roughness height  $Z_0$  of these surfaces is about 0.1 to 1 cm (Sutton et al., 1979). Fortunately, a surface having these values of  $Z_0$  requires a threshold wind speed at the top of the boundary layer  $V_{gt}$  that is almost identical to the one needed for a surface containing only sand grains (see Fig. 3 of Pollack et al., 1976a, b). Thus, good estimates of  $V_{gt}$  at the lander sites may be made by multiplying the laboratory threshold friction velocities by the ratio of  $V_{gt}/u_*$  appropriate for a sand only case ( $\sim 50$ ). This conversion is indicated by the Case 1 scale of Figure 5. Analysis of the Viking meteorology results suggest that the ratio,  $r$ , of the wind speeds measured by the Viking Meteorology Instrument to those at the top of the boundary layer equals about 0.4 (Leovy and Zurek, 1979).

We are now in a position to compare the velocities measured in the Viking meteorology experiment with threshold values for the optimum grain size, i.e., the grain size easiest to move ( $\sim 100 \mu\text{m}$ ). During the early portion of the Viking mission (northern hemisphere summer), the surface pressures at the landers was about 7.5 mb, while close to the time of the second global dust storm (southern hemisphere summer) the pressure had increased to about 9.5 mb (Ryan et al., 1978). Using the results of Figure 5 and a scale factor of 20 to convert friction velocities to velocities at the height of the meteorology sensors we estimate that the measured wind had to exceed about 30 and 25 m  $\text{s}^{-1}$ , respectively, for saltation to occur. During the summer season in the northern hemisphere, the measured wind speed did not exceed  $10 \text{ m s}^{-1}$  at either lander (Hess et al., 1976a, b) and hence saltation should not have occurred, in accord with lander camera observations (Mutch et al., 1976a, b). The strongest winds measured to date were observed at the first lander site shortly after the onset of the second global dust storm. Sustained wind speeds of  $18 \text{ m s}^{-1}$  were recorded, with peak gusts of up to  $28 \text{ m s}^{-1}$  (Ryan et al., 1978). Thus, the winds came quite close to reaching threshold conditions. This prediction is in reasonable accord with lander camera results. Movement did occur in sand piles placed on top of the lander, where threshold conditions are lower, but no alteration was observed to occur on the surface, except for a few isolated places (Sagan et al., 1977 and Jones et al., 1979). Conceivably, during martian years of somewhat enhanced global dust storm activity, the saltation threshold is exceeded at the lander sites, especially Viking Lander 1.

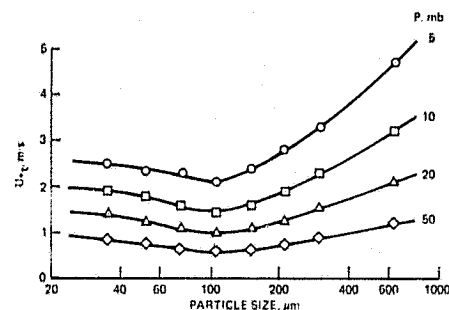


Figure 4. Friction threshold velocity as a function of particle size as determined in wind tunnel tests using ground walnut shell and 95 percent  $\text{CO}_2$  air mixture.



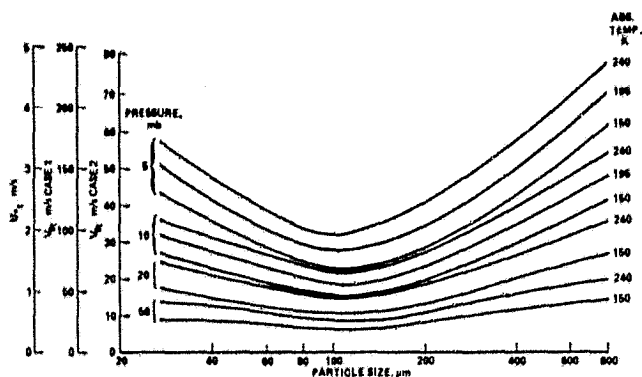


Figure 5. Particle threshold curves as a function of particle size for martian surface pressures and higher, and for representative martian temperatures. Case 1 scale is free stream velocity (above boundary layer) for winds blowing over a flat surface of erodible grains; Case 2 surface containing cobbles and small boulders.

**Acknowledgment.** This work was supported by the Planetary Geology Program Office, National Aeronautics and Space Administration.

#### References

- Adlon, G. L., R. K. Weinberger, and D. R. McClure, Planetary environment simulation: Martian sand and dust storm simulation and evaluation, NASA CR-66882, 1969.
- Arvidson, R. E., Aeolian processes on Mars: Erosive velocities, settling velocities, and yellow clouds, *Geol. Soc. Am. Bull.* 83, 1503-1508, 1972.
- Bagnold, R. A., *The Physics of Blown Sand and Desert Dunes*. London: Methuen, 1941.
- Barr, P. K., Calculation of skin-friction coefficients for low-Reynolds-number turbulent boundary layer flows, unpubl. M.S. Thesis, University of California, Davis, California, 1979.
- Chang, T. S., W. C. Lucas, and W. W. Youngblood, Laboratory simulation of the Mars atmosphere: A feasibility study, NASA CR-61188, 1968.
- Coles, D. E., The turbulent boundary layer in a compressible fluid, Rand Corp. Report 403-PR, Santa Monica, California, 1962.
- Greeley, R., B. R. White, R. N. Leach, J. D. Iversen, and J. B. Pollack, Mars: Wind friction speeds for particle movement, *Geophys. Res. Letters*, 3, 417-420, 1976.
- Greeley, R., B. R. White, J. B. Pollack, J. D. Iversen, and R. N. Leach, Dust storms on Mars: Considerations and simulations, NASA TM-78423, 1977.
- Hess, S. L., R. M. Henry, C. B. Leovy, J. A. Ryan, J. E. Tillman, T. E. Chamberlain, H. L. Cole, R. G. Dutton, G. C. Greene, W. E. Simon, and J. L. Mitchell, Mars climatology from Viking after 20 sols, *Science*, 194, 78, 1976a.
- Hess, S. L., R. M. Henry, C. B. Leovy, J. L. Mitchell, J. A. Ryan, and J. E. Tillman, Early meteorological results from the Viking 2 lander, *Science*, 184, 1352, 1976b.
- Iversen, J. D., R. Greeley, J. B. Pollack, and B. R. White, Simulation of martian aeolian phenomena in the atmospheric wind tunnel, NASA SP-336, 191-213, 1973.
- Iversen, J. D., J. B. Pollack, R. Greeley, and B. R. White, Saltation threshold on Mars: The effect of interparticle force, surface roughness, and low atmospheric density, *Icarus*, 29, 381-393, 1976.
- Jones, K. L., R. E. Arvidson, E. A. Guinness, S. L. Bragg, S. D. Wall, C. E. Carlston, and D. G. Pidek, One Mars year: Viking lander imaging observations, *Science*, 204, 799-806, 1979.
- Leovy, C. B. and R. W. Zurek, Thermal tides and martian dust storms: Direct evidence for coupling, *J. Geophys. Res.*, 84, 2956-2968, 1979.
- Mutch, T. A., A. B. Binder, F. O. Huck, E. C. Levinthal, S. Liebes Jr., E. C. Morris, W. R. Patterson, J. B. Pollack, C. Sagan, and G. R. Taylor, The surface of Mars: The view from the Viking 1 lander, *Science*, 193, 791, 1976a.
- Mutch, T. A., S. V. Grenander, K. L. Jones, W. Patterson, R. E. Arvidson, E. A. Guinness, P. Avrin, G. E. Carlston, A. B. Binder, C. Sagan, E. W. Dunham, P. L. Fox, D. C. Pieri, F. O. Huck, C. W. Rowland, G. R. Taylor, S. P. Wall, R. Kahn, E. C. Levinthal, S. Liebes Jr., R. B. Tucker, E. C. Morris, J. B. Pollack, R. S. Saunders, and M. R. Wolf, The surface layer of Mars: The view from the Viking 2 lander, *Science*, 194, 1277, 1976b.
- Patel, V. C., Calibration of the Preston tube and limitations on its use in pressure gradients, *J. Fluid Mech.*, 23, 185-208, 1965.
- Pollack, J. B., R. Haberle, R. Greeley, and J. D. Iversen, Estimates of the wind speeds required for particle motion on Mars, *Icarus*, 29, 395-417, 1976a.
- Pollack, J. B., C. B. Leovy, Y. H. Mintz, and W. VanCamp, Winds on Mars during the Viking season, predictions based on a general circulation model with topography, *Geophys. Res. Letters*, 3, 479-482, 1976b.
- Ryan, J. A., R. M. Henry, S. L. Hess, C. B. Leovy, J. E. Tillman, and C. Walcek, Mars meteorology: Three seasons at the surface, *Geophys. Res. Letters*, 5, 715, 1978.
- Sagan, C., D. Pieri, P. Fox, R. E. Arvidson, and E. A. Guinness, Particle motion on Mars inferred from the Viking lander cameras, *J. Geophys. Res.*, 82, 4430-4438, 1977.
- Sagan, C. and J. B. Pollack, Windblown dust on Mars, *Nature*, 223, 791-794, 1969.
- Sutton, J. L., C. B. Leovy, and J. E. Tillman, Diurnal variations of the martian surface layer meteorological parameters during the first 45 sols at the two Viking lander sites, *J. Atmos. Res.*, in press, 1979.
- White, B. R., Low-Reynolds-number turbulent boundary layer flows, paper presented at the ASME 21st Annual Meeting, *Symposium of Turbulent Boundary Layers*, Niagara Falls, New York, June, 1979.

(Received September 11, 1979;  
accepted October 18, 1979.)

**MARS: PRELIMINARY ESTIMATES OF RATES OF WIND EROSION BASED ON LABORATORY SIMULATIONS.** *R. Greeley and S.H. Williams, Department of Geology and Center for Meteorite Studies, Arizona State University, Tempe, AZ 85281.*

Ample evidence exists for aeolian erosion and deposition on Mars. Prior to Viking, relatively high rates of erosion by windblown particles had been predicted (1), based partly on the observations of frequent dust storms and the fact that the particles should be highly energetic because they would be driven at high velocities by the order-of-magnitude stronger winds required to set them into motion. Furthermore, the decrease in possible atmospheric "cushioning" in the low density atmosphere of Mars might enhance the rate of erosion (2). However, one of the surprises from the Viking Mission was the apparent low rate of wind erosion evidenced at the Viking landing sites (3). A recent estimate (4) suggests a rate on the order of a millimeter per million years based on preservation of surface features and ages derived from impact crater statistics.

In order to determine rates of aeolian erosion on Mars, three general parameters must be known: 1) erosive effectiveness of windblown particles under martian conditions, 2) material properties of martian rocks and minerals as related to resistance to aeolian erosion, and 3) near-surface meteorological conditions on Mars (wind speeds, duration, etc.). The first two general parameters can be investigated in wind tunnels and through other laboratory simulations; the latter parameter can be obtained from the Viking meteorology experiments, at least for the areas around the landing sites. In this report, we present preliminary data from laboratory simulations of aeolian erosion on Mars and combine the results with early Viking meteorology data to estimate a rate of erosion.

The Rotating Arm Mars Erosion Device (RAMED) consists of a holder for various rock samples at the end of a rotating arm and a sand hopper from which sand can be dropped into the path of the target (fig. 1). Atmospheric pressure and composition, impact particle size and quantity, target composition, and impact velocity can all be controlled. The sample is weighed before and after each run, the data being plotted as target mass lost per impacting mass, a unitless parameter, as a function of impact velocity and rock type. Quartz sand was used as the impacting material. Its size range was 120-180 microns, the size most easily moved by martian winds (5). RAMED results for a variety of rock types are shown in fig. 2; as expected, different rocks have different resistances to erosion, reflecting grain and crystal size, bonding, composition, etc., with rhyolite and obsidian being relatively resistant, and sandstone being relatively susceptible to erosion. For particles in the 120-180 micron size range impacting at relatively low velocities ( $\sim 10$  m/s), the mass lost from the target rock is on the order of  $10^{-4}$  of the impacting mass and  $10^{-6}$  of the impacting kinetic energy. An approximate erosion rate can now be calculated using the equations presented by Sagan (1). However, several values must be changed to reflect Viking data and the laboratory simulations. The frequency of winds of sufficient speed to cause particle saltation is several orders of magnitude smaller than that used by Sagan (6). In addition, the mass lost from the target per unit impacting KE is on the order of  $10^{-6}$ , rather than  $10^{-4}$ . A preliminary determination of flux for a saltating cloud was obtained at the MARSWIT facility in 1977 (7). When the results are scaled to Mars, the number density of particles becomes approximately  $10^{-5}$  particles  $\text{cm}^{-3}$ . With these refined values, the rate of erosion is found to be about a millimeter per million years and is in general agreement with the estimate of Arvidson *et al* (4), based on a completely different technique.

## **WIND EROSION ON MARS**

**Greeley, R. et al.**

The result presented here is preliminary. Additional experiments are in progress to refine these data; it is also hoped that additional meteorological data will become available regarding wind strengths and frequencies.

### **REFERENCES**

- (1) Sagan, C. (1973) *J. Geophys. Res.*, 78, 4155-4151.
- (2) McCauley, J.F. (1973) *J. Geophys. Res.*, 78, 4123-4138.
- (3) Binder, A.B., et al. (1977) *J. Geophys. Res.*, 82, 4439-4451.
- (4) Arvidson, R., et al. (1978) in press.
- (5) Greeley, R., et al. (1976) *Geophys. Res. Lett.*, 3, 417-420.
- (6) Hess, S.L., et al. (1977) *J. Geophys. Res.*, 82, 4559-4574.
- (7) The Martian Surface Wind Tunnel (MARSWIT) is a facility at NASA-Ames Research Center capable of operating in the wind velocity range and atmospheric pressures comparable to Mars. Saltating flux experiments were conducted at one atmospheric pressures by J. Burt in 1977.

**WIND EROSION ON MARS**  
**Greeley, R. et al.**

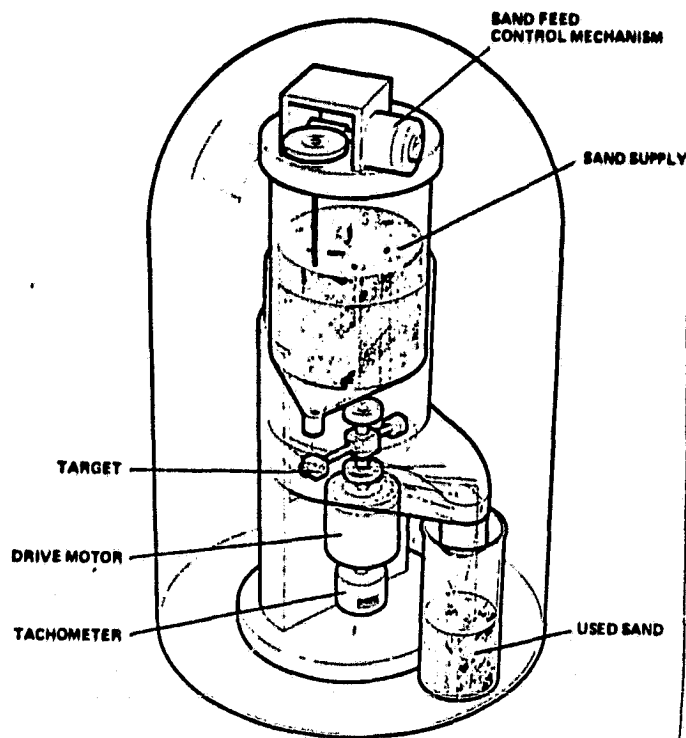


Figure 1 RAMED (Rotating Arm Martian Erosion Device) used for simulation of aeolian erosion on Mars. Device is about 0.5 m high and is placed in a bell jar (as depicted) for experiments run at low pressure and in a CO<sub>2</sub> atmosphere. Target (rock sample) rotates to impact sand grain at a controlled velocity.

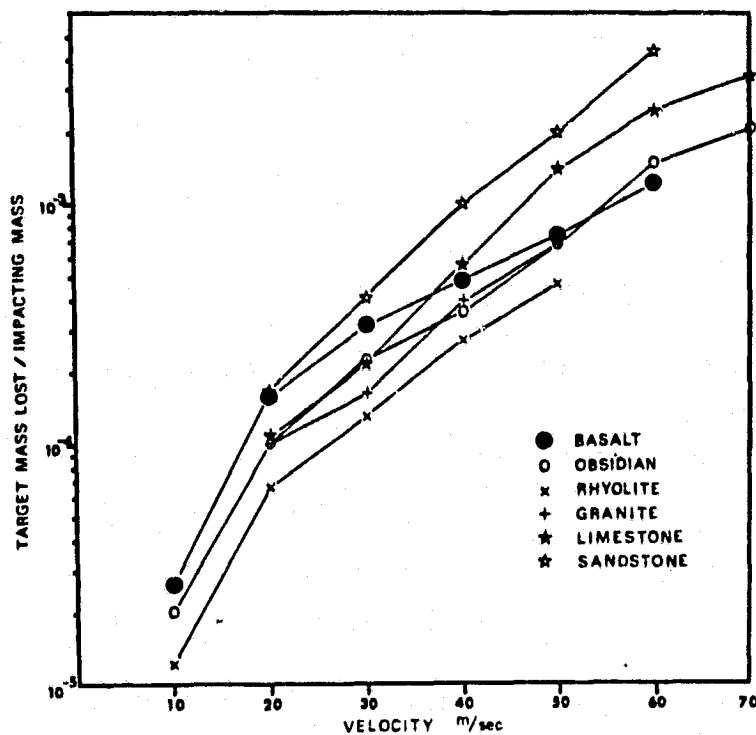


Figure 2 Erosion of 6 rock types as a function of simulated aeolian abrasion. Tests were done at martian pressure (~ 3mb). The impactors were quartz sand in the 120-180 micron diameter range.

## "STEAM" INJECTION OF DUST ON MARS: LABORATORY SIMULATIONS

Greeley, R., Center for Meteorite Studies, Department of Geology, Arizona State University, Tempe, AZ 85281 and Leach, R., University of Santa Clara at NASA-Ames Research Center, Moffett Field, CA 95035

One of the puzzles regarding the aeolian regime on Mars concerns the mechanisms for initiation of the frequent dust storms. Estimated particle size in the dust storms is a few microns or less (Pollack *et al.*, 1977, and others); yet predictions of threshold wind speeds needed to move particles of this size on Mars are in excess of  $250 \text{ m s}^{-1}$  (Greeley *et al.*, 1976) for winds blowing across a smooth bed of uniform size particles, and it is doubtful that much, if any, dust is raised in this manner. The optimum particle size for movement by winds is about  $160 \mu\text{m}$  which has a much lower threshold wind friction velocity ( $\sim 25$  to  $75 \text{ m s}^{-1}$ ); once these grains begin saltating they could be expected to set smaller grains into motion upon impact. However, even these winds seem to be rather infrequent, at least at the Viking landing sites. Thus, there may be some mechanism other than wind alone to initiate dust movement. Such a mechanism was proposed by Johnson *et al.* (1975) involving injection of dust into the atmosphere resulting from desorption in response to heating of adsorbed  $\text{CO}_2$  on grains. A similar mechanism could occur involving water; Huguenin *et al.* (1979) have shown that substantial amounts of water vapor could be released to the atmosphere and have suggested that some of the "blue clouds" observed on Mars are water clouds.

We have conducted exploratory experiments in the laboratory to study the effects of water vaporization on the movement of fine-grained material. Experiments were performed in both a bell jar and in a low atmospheric pressure wind tunnel using a range of particle compositions and sizes, including: fine silt ( $10 \mu\text{m}$ ), talc ( $13 \mu\text{m}$ ), loess ( $20 \mu\text{m}$ ), quartz ( $23$ – $44 \mu\text{m}$ ), walnut shells ( $61$ – $88 \mu\text{m}$ ), and poorly sorted calcite grains ( $12$ – $1000 \mu\text{m}$ ) (walnut shells having been used previously in threshold tests, see Greeley *et al.*, 1977). In bell jar tests, as the atmospheric pressure was reduced below 10 mb (temperature  $\sim 24^\circ \text{C}$ ) adsorbed water vaporized and ejected particles by one of two processes: 1) vent holes and fissures would develop, followed by a fountainlike spray of particles as high as 20 cm above the surface, or 2) violent "eruptions" occurred in a boiling fashion (similar to the mechanism described by Johnson *et al.*, 1975). The smaller the grain size the more violent the eruption, although some activity increased with depth of particle bed, with 20 cm high activity occurring for beds 10 cm deep; some activity was also observed in beds as shallow as 1 mm. The amount of adsorbed water also affected activity, with ejection occurring with water contents as low as 0.75% by weight.

Similar effects were observed in tests conducted in the wind tunnel. However, it was noted in some experiments that the particle bed remained stable until a low velocity wind passed over the surface at which time injection was "triggered". Although there is no clear explanation for this effect, the triggering could be related to slight differences in pressure resulting from the wind.

Figure 1 shows sequential pictures of a silt bed in the wind tunnel; as the pressure was reduced, at about 10 mb the surface developed numerous

irregular fissures in response to outgassing water vapor. The surface was then subjected to wind and the fissured surface began to erode as the wind picked up crust-like sections of the silt; the wind speed was  $\sim 25 \text{ m s}^{-1}$ , substantially lower than "normal" threshold for undisturbed silt. Evidently, the fissuring of the silt bed sufficiently roughened the surface to lower the threshold speed. On Mars, variations in surface temperature and pressure through the critical range for water vaporization may produce "jetting" of particles into the atmosphere, or disturb the surface to allow small particles to be set into motion by winds otherwise much too slow for "normal" threshold.

#### References

Greeley, R., *et al.* (1976) *Geophys. Res. Letter*, 3, 417-420.

Greeley, R., *et al.* (1977) NASA TM-78423, 29p.

Huguenin, R., *et al.* (1979) NASA Conf. Publ. 2072, 40. (and this issue).

Johnson, W., *et al.* (1975) *Icarus* 26, 441-443.

Pollack, J., *et al.* (1977) *J. Geophys. Res.*, 82, 4479-4496.

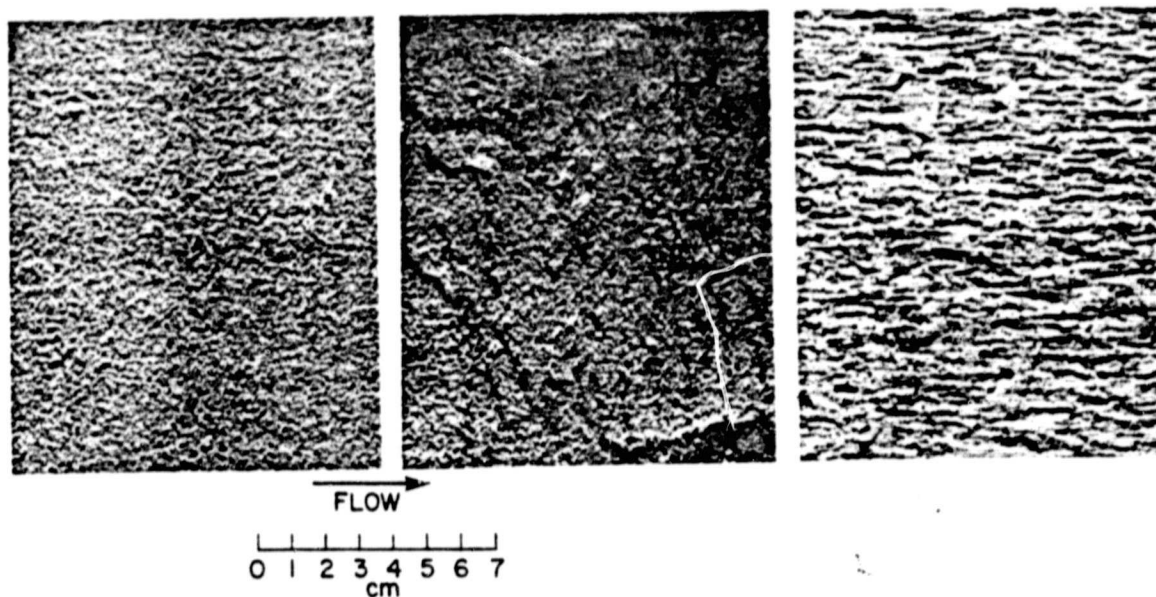
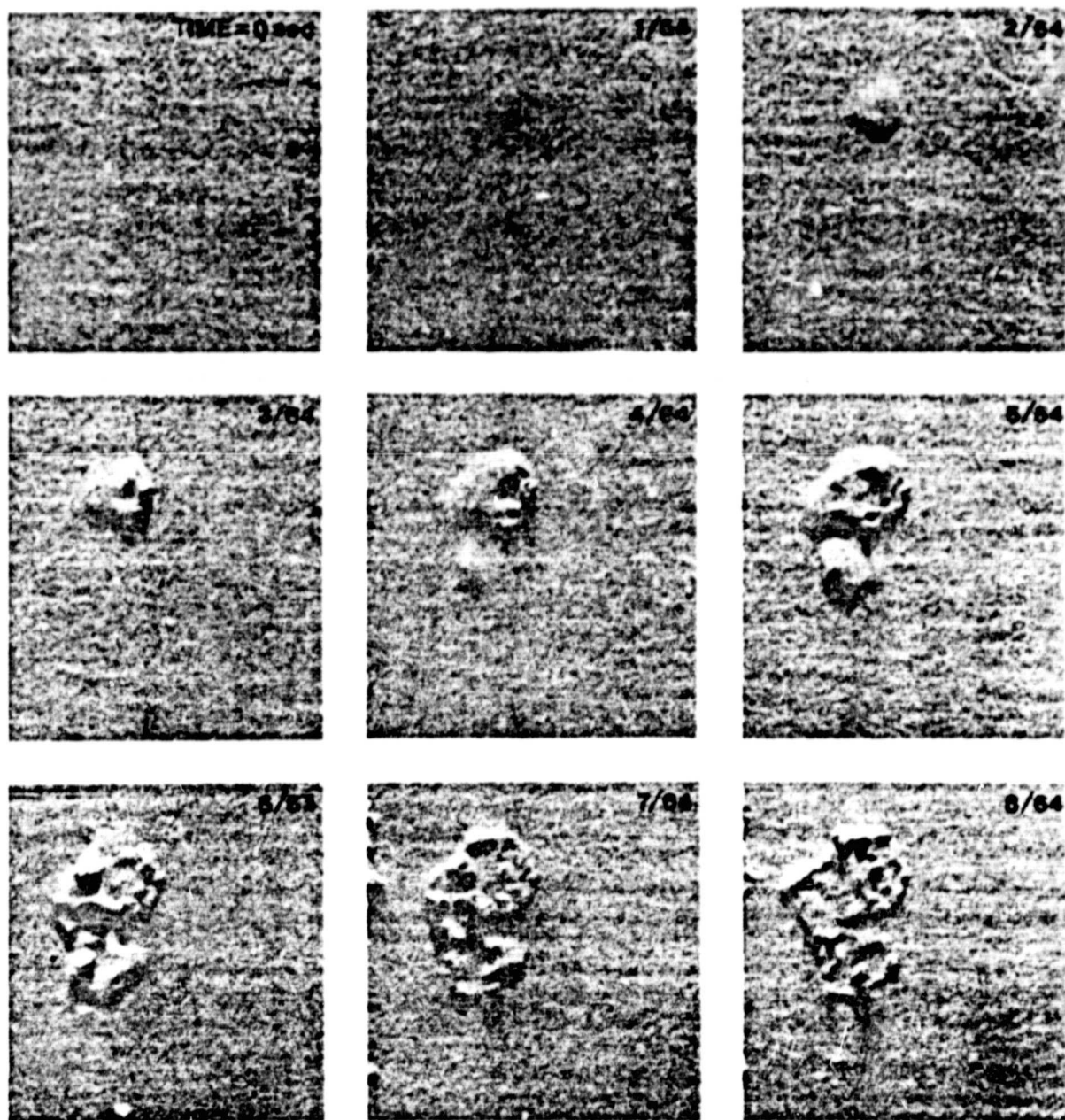


Figure 1. Series of photographs of fine silt particles in a low pressure wind tunnel; a) bed prior to experiment; b) fissured surface that occurred as atmospheric pressure in wind tunnel chamber was reduced to about 10 mb; c) surface eroded by  $25 \text{ m s}^{-1}$  wind.

Figure 2. Sequential frames showing injection of fine grained particles as a result of water vaporization at about 10 mb pressure.



PRECEDING PAGE BLANK NOT FILMED

Material Removal and Production of Fines During Aeolian Erosion of Minerals:  
Mars and Earth

T. R. McKee and R. Greeley, Geology Department and Center for Meteorite Studies and D. H. Krinsley, Geology Department, Arizona State University, Tempe, AZ 85281

Aeolian erosion, or comminution of rock and particle surfaces by windblown materials is an important process on Earth and certain other planets. Laboratory simulations under various conditions are being utilized in a coordinated program to study a wide range of aeolian processes from geomorphology on a megascopic scale to impact erosion on a microscopic scale. Although general concepts of aeolian erosion have been developed, the mechanisms involved in material removal at microscopic scales and subsequent production of fine-grained particulate are unknown. The value to planetary geology of an analytical impact erosion model is its capability to predict trends in aeolian erosion when the properties of the materials involved or the existing erosion conditions are changed due to new or reinterpreted data. At present there have been too few observations of impact erosion under closely controlled conditions to allow development of a complete analytical model.

In order to develop a general understanding of aeolian erosion, single and multiple impacts of fine-grained material upon rock surfaces are being studied at a range of velocities characteristic of Earth and Mars (8 - 107 m/s). Quartz is one of the most common aeolian materials on Earth and can be used as a control in a model development program; in addition, its material properties and characteristics are well known. In one portion of this study, monocrystalline quartz plates and quartz single crystals were eroded by quartz sand (125-180  $\mu\text{m}$  dia.) in a slinger erosion device at known impact velocities and impact angles<sup>1</sup>. Individual erosion pits were produced on rhombohedral faces of quartz single crystals at about a 50° impact angle and impact velocities of 16 m/s and 75 m/s. Two types of erosion pits were observed: 1) shallow arc shaped pits (Fig. 1a,b,c) and 2) pits of complex morphology (Fig. 2). At 16 m/s shallow pits (Figs. 1a,b) with an average diameter of 15  $\mu\text{m}$  predominate, whereas at 75 m/s the average pit diameter is 30  $\mu\text{m}$  and deep, complex pits predominate. The ideal single impact feature for a brittle material is characterized by a central deformation zone (impact site) surrounded by a shallow network of radial and circular microcracks<sup>2</sup> (Fig. 3) which are modified by the impact angle (Fig. 4) such that an incomplete circle is obtained, and by the crystalline structure of the sample such that in some cases the circular outline becomes polyhedral (Fig. 1c). If the erosion pits in Fig. 1b and 1c were complete, they would both be about 45  $\mu\text{m}$  in diameter, producing several flat chips 10-20  $\mu\text{m}$  in diameter and 1-2  $\mu\text{m}$  thick. At higher velocities, the central zone of deformation (about 10  $\mu\text{m}$ ) would produce a large number of clay-sized particles. The Argonne slinger erosion device unfortunately was not designed for collection of the clay-sized particles, however this capability will exist with the ASU machine. Alternately clay-sized particles produced by erosion in a paddle wheel device were studied by transmission electron microscopy (TEM) and selected area electron



diffraction (SAED). Submicron particles produced by erosion at 40 m/s showed evidence of plastic deformation, exhibiting asterism in SAED patterns (Fig. 5) which was not present in the ground quartz used as starting material.

Plots of quartz erosion rates versus impact angle exhibit maxima near 90° which is characteristic of brittle fracture, whereas ductile fracture would have a maximum at about 18° (Fig. 6)<sup>3</sup>. The surface textures produced exhibit angular pits surrounded by irregular, offset ridges (Fig. 7, 8a). A model for removal of surface material is simply an extension of the complex erosion pits produced by interaction of several microcrack systems. Material is removed from the surface by the interaction of microcracks radiating from a network of adjacent impact sites (circles, Fig. 7) and complex, blocky or flat chips 10-30 μm in diameter are produced. At 75 m/s many of the ridge-top surfaces appear to be plastically deformed and probably represent remnant portions of the central zone of deformation of impact sites (Fig. 8a,b).

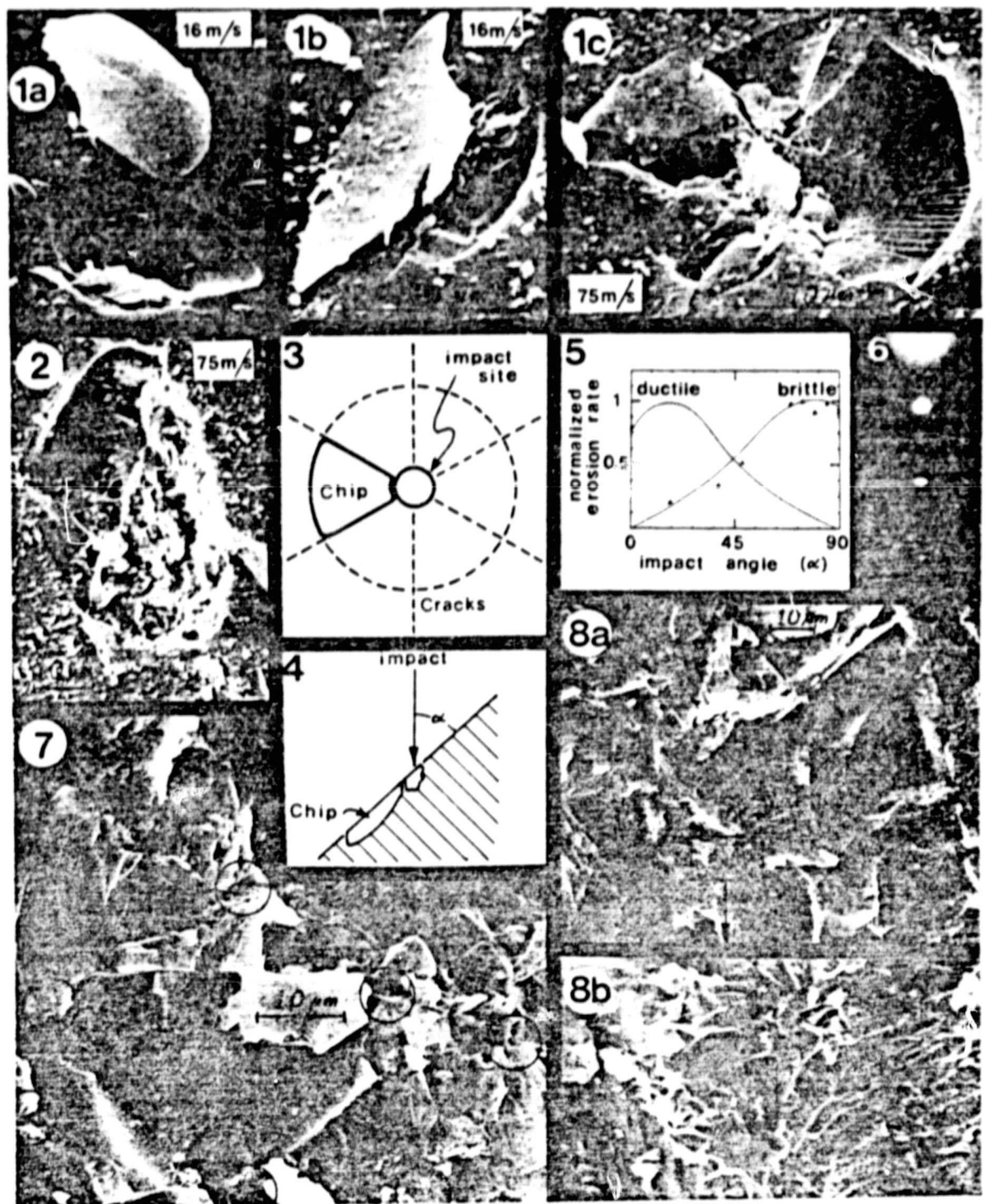
In summary, it has been shown that aeolian surface textures on quartz are produced by interaction of microcracks radiating from individual impact sites in a manner characteristic of brittle fracture. In addition, a mechanism is suggested for the production of fine silt and clay-sized material, depending upon the impact velocities involved. At characteristic earth velocities silt would probably be the dominant product whereas at martian velocities and higher earth velocities both silt and clay-sized material would be produced. At higher velocities the clay-sized material and some sand and rock surfaces would be plastically deformed, altering their bulk response to geochemical and biochemical environments.

#### References:

1. McKee, T. R., Greeley, R., and Krinsley, D. H., 1979, Simulated aeolian erosion of quartz: Proc. 37th Ann. Electron Microscopy Soc. of Am., p. XXX.
2. Lawn, B. R., Swain, M. V., and Phillips, K., 1975, On the mode of chipping fracture in brittle solids: J. Mat. Sci. 10:1236-1239.
3. Finnie, I., 1960, Erosion of surfaces by solid particles: Wear 3:87-103.

#### Acknowledgments:

Appreciation is expressed to the Mech. Prop. Group, Argonne Nat. Lab. for use of the slinger erosion device (and advice during construction of a similar device at ASU) and to A. Turner, J. Routbort, T. Kosel, R. Scattergood and L. Funk for valuable discussion. This research was supported by NASA Consortium Agreement #NCA2-OR035-801 and #NCA2-OR035-901 through the Planetary Geology Program.



CALIBRATION OF THE MARSWIT TUNNEL FOR DETERMINATION OF PARTICLE THRESHOLD SPEEDS,

B. R. White, Department of Mechanical Engineering, University of California, Davis, CA 95616; R. N. Leach, University of Santa Clara, NASA-Ames Research Center, Moffett Field, CA 94035; J. D. Iversen, Department of Aerospace Engineering, Iowa State University, Ames, IA 50011; R. Greeley, Department of Geology and Center for Meteorite Studies, Arizona State University, Tempe, AZ 85218.

This abstract describes the procedure and results established in calibration of the low pressure open circuit wind tunnel (MARSWIT, described in Greeley *et al.*, 1977) for determination of threshold friction speeds. The wind-tunnel test procedure was as follows: A bed of uniform-sized particles was placed in the wind-tunnel test section and the surface was smoothed. For each test a 2.5 meter long bed of material was used, as previous tests showed (Greeley *et al.*, 1977) that a bed of this length would give very nearly the same results as an infinitely long bed whereas shorter beds resulted in increased saltation threshold values. The tunnel is located inside a large vacuum chamber which was evacuated to about 4 mb pressure using "Earth" air. The tunnel was then started and the wind speed gradually increased until saltation threshold was reached. The tunnel was stopped and started several times at each test condition to give a number of data points. Three separate methods were used to determine saltation threshold: (1) A high resolution closed-circuit television system was used to observe the particle movement directly; (2) A laser-photocell system indicated saltation by the attenuation of the signal due to particles interrupting the laser beam; and (3) An electrostatic detector measured the current produced by saltating particles impinging on the detector element. For most experiments all the systems were used concurrently to detect saltation, with the electrostatic system being more sensitive for small particles and the television and laser system more sensitive for the larger particles.

The chamber was then filled with CO<sub>2</sub> to a pressure of about 80 mb giving a 95 percent CO<sub>2</sub> and 5 percent air mixture. Threshold tests were run at various pressures as the chamber pressure was again reduced to 4 mb. Finally, the chamber was purged with air and pumped to 4 mb for the third time. Threshold speeds were again taken with air as the working fluid, as the chamber was step-filled to atmospheric pressure. With this technique it was possible to compare a particular bed of material with all conditions nearly identical except that the working fluid was changed from air to CO<sub>2</sub> and back to air. By comparing the initial air data with the final air data a good estimation of the repeatability of the data could be made.

The critical measurements in the wind tunnel are the differential pressure ( $\Delta p$ ) between the total pressure ( $p_t$ ) and the static pressure ( $p_s$ ) at the tunnel centerline, and the chamber pressure and temperature. The tunnel centerline wind velocities can then be calculated from these measurements, as well as the friction velocity ( $u_*$ ) for a given bed of materials taking into account the boundary layer profile and the surface roughness.

Time-averaged boundary layer velocity profiles were determined from differential pressure measurements between static Pitot tubes and a Pitot tube that was transversed through the boundary layer. The tests showed the boundary flow to be essentially steady, two-dimensional, constant-property (i.e., maintaining a constant chamber pressure), and to have constant free-stream velocity turbulent flow over the tunnel wall. A zero-pressure-gradient flow was achieved by increasing the roof height with increasing downstream distance (thereby expanding the cross sectional area); the zero-pressure-gradient was verified by static pressure measurements at several positions in the tunnel. A naturally turbulent boundary layer was developed

for most of the flow conditions; however, at the lower pressures it was necessary to trip the boundary layer by placing small pebbles on the tunnel floor in the entrance section of the tunnel. The test section was more than 25 boundary-layer thickness-lengths from the pebbles placed upstream, insuring a fully developed turbulent core region at low pressures.

The data were reduced taking into account Mach number and slip flow effects in the velocity determination. Each profile was numerically curve fitted by means of a multi-piecewise cubic spline technique.

For the turbulent boundary layer the value of the friction speed  $u_*$  is dependent on the value of the momentum thickness Reynolds number

$$Re_\theta = \frac{u_\infty \theta}{\nu}$$

when  $u_\infty$  is the free-stream wind-tunnel speed,  $\nu$  is the kinematic viscosity, and  $\theta$  is the momentum-deficit thickness. The momentum-deficit thickness is defined as the thickness of the layer as measured from the wall of an external stream (at constant speed  $u_\infty$ ) containing a momentum flux equal to the loss of momentum flux due to the presence of the wall. It is convenient to define the momentum-deficit thickness  $\theta$  in terms of mean velocity profiles as

$$\theta = \int_0^\delta \left[ \frac{u}{u_\infty} \right] \left( 1 - \frac{u}{u_\infty} \right) dy$$

where  $\delta$  is the boundary layer height at which the value of velocity  $u$  is 99 percent that of  $u_\infty$ , and  $y$  is the vertical height. The momentum thicknesses were determined from integrating the resultant curve fit by a numerical quadrature technique.

An analysis of the zero-pressure-gradient turbulent boundary layer for low Reynolds numbers has been made by Coles (1962); from this work the surface shear stress  $\tau_0$  can be determined from the velocity profiles obtained in the wind tunnel. This is accomplished by assuming that the velocity obeys the logarithmic law

$$\frac{u}{u_*} = \frac{1}{\kappa} \ln \frac{u_* y}{\nu} + C,$$

for the wall region ( $y/\delta < 0.2$ ) excluding the viscous sublayer. In this study,  $\kappa = 0.418$  and  $C = 5.45$ , as determined by Patel (1965). Converting to  $\log_{10}$  gives

$$\frac{u}{u_*} = 5.5 \log_{10} \frac{u_* y}{\nu} + 5.45$$

The ratio  $u_*/u_\infty$  is well fit by the empirical equation

$$\frac{u_*}{u_\infty} = 0.702 (\log_{10} Re_x)^{-1.59}$$

as shown by Figure 1. In this equation the relationship is presented as a function of  $Re_x$ , the Reynolds number based on the distance from the beginning of the wind tunnel to the test point. For flows with lower values of  $Re_\theta$  ( $Re_\theta < 600$ ) the ratio  $u_*/u_\infty$  becomes a constant value of approximately 0.049. This is the maximum

value that  $u_* / u_{\infty}$  can obtain in a turbulent boundary layer at low Reynolds numbers (White, 1979, and Barr, 1979). For values of  $Re_{\theta}$  less than 425 the boundary layer flow is laminar and is of no importance in flows of saltating particles.

#### REFERENCES

- Barr, P.K., "Calculation of friction factors for low Reynolds number turbulent boundary layer flows", M.S. Thesis, Library, University of California, Davis, California, 1979.
- Coles, D.E., "The turbulent boundary layer in a compressible fluid", Rand Report 403-PR, 1962.
- Greeley, R., White, B.R., Pollack, J.B., Iversen, J.D., and Leach, R.N., "Dust storms on Mars: Considerations and simulations", NASA Technical Memorandum 78423, December, 1977.
- Patel, V.C., "Calibration of the Preston tube and limitations on its use in pressure gradients", Journal of Fluid Mechanics, Vol. 23, 1965, pp. 185-208.
- White, B.R., "Low-Reynolds number turbulent boundary layers", ASME, Symposium on Turbulent Shear Flows, Niagara Falls, New York, June 1979.

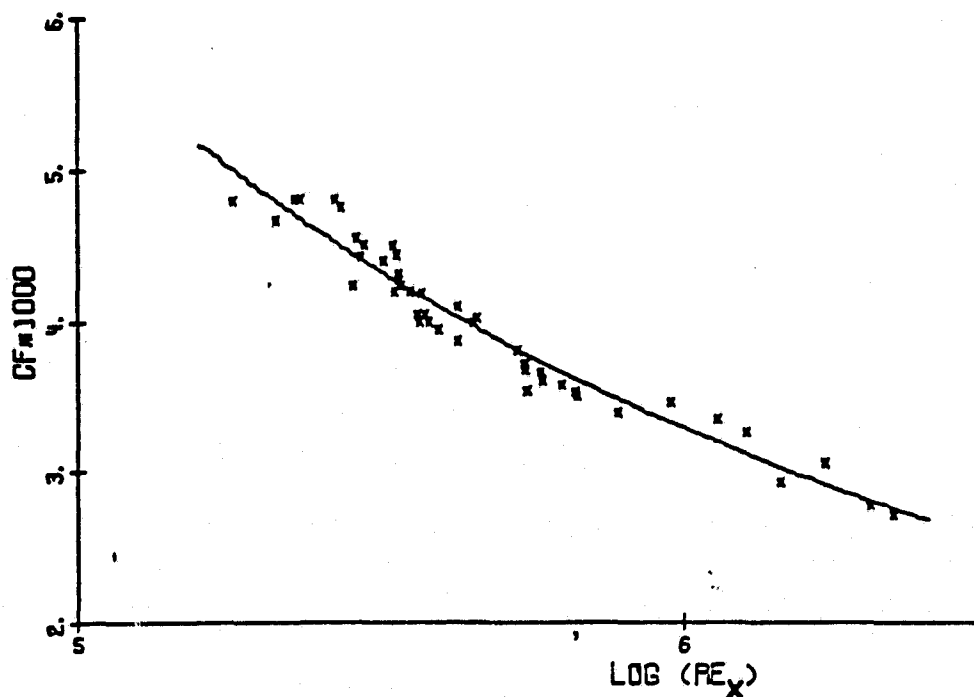


FIGURE 1 The skin-friction coefficient as function of Reynolds number  $Re_x$ .

## WIND EROSION ON MARS: AN ESTIMATE OF THE RATE OF ABRASION.

S. H. Williams and R. Greeley, Department of Geology, Arizona State University, Tempe, Arizona 85281.

Preliminary estimates of aeolian abrasion rates on Mars have been reported previously (1), and the general procedures and approach are presented by Krinsley et al. (2). Earth based observations and the global dust storm seen by Mariner 9 led Sagan (3) to predict extremely large aeolian abrasion and deflation rates, based on saltation physics and some assumptions of martian environmental conditions. This rapid rate is at odds with constraints placed upon it by observations of surface features made from Viking images (4,5). Refinement of Sagan's calculation was made based on laboratory studies and Viking data resulting in an aeolian abrasion rate more compatible with observations of the surface (1). However, values for the parameters in the calculation are open to question, and have led to additional work using a different approach, as reported here.

The mass rate of aeolian abrasion is the product of three basic parameters:

- 1)  $S_A$  The susceptibility of a given material to abrasion measured in grams target lost per grams impacting mass.
- 2)  $q$  The mass flux of impacting material on the target, measured in grams impacting per square centimeter of target per second;  $q$  is a function of wind speed and height above a surface roughness.
- 3)  $f$  The frequency of winds of saltation-strength.

$$\text{Mass rate of abrasion} = S_A \cdot q \cdot f; \text{ units: gm cm}^{-2} \text{ sec}^{-1}$$

The first parameter,  $S_A$ , is measured in the laboratory using abrasion devices that simulate natural abrasion under martian conditions (6). The second parameter,  $q$ , can be measured for terrestrial environmental conditions in the field and in wind tunnels. An extrapolation of  $q$  thus determined to martian conditions is possible using equations developed by White (7) and can be compared to  $q$  measured under simulated martian conditions in MARSWIT, a low pressure wind tunnel at NASA-Ames Research Center. An estimate of the third parameter can be made from Viking meteorological observations. The only other input required for the rate calculation is the relationship between wind velocity and sand velocity in a saltation cloud.

The values for all three parameters are currently being refined; however, a first-order estimate of the abrasion rate on Mars can be made, based on the following assumptions:

- 1) Impactors are quartz sand similar to those used in the abrasion devices.
- 2) There is sufficient sand on the martian surface to allow a full saltation curtain to develop, as in wind tunnel experiments.
- 3) Rocks on Mars have similar abrasion susceptibilities as those on Earth of assumed similar composition and texture.
- 4) The present meteorological conditions as measured by the Viking Lander on Mars are similar to those in the past.

## WIND EROSION ON MARS: RATE OF ABRASION ESTIMATE

Williams and Greeley

Values for these parameters can be estimated as follows:

Parameter	Typical Value	Source	Reference
$S_A$	$10^{-4}$	Abrasion machines	1,8
$q$	0.1	Earth wind tunnel extrapolated to Mars	7,9
$f$	A maximum of $10^{-2}$ , more likely $10^{-3}$	Viking observation	10

$$\text{Mass Rate of Abrasion} = (10^{-4})(10^{-1})(10^{-3}) = 10^{-8} \text{ gm cm}^{-2} \text{ sec}^{-1}$$

$$\text{Depth Rate of Abrasion} = \frac{\text{mass rate}}{\text{target density}} = \sim 4 \cdot 10^{-9} \text{ cm sec}^{-1}$$

The results in an abrasion rate of 0.1 centimeters per year (1000 meters per million years). Refinement of the measurements of  $S_A$ ,  $q$  and  $f$  will increase the accuracy of this rate, however, most of the values are within order of magnitude and yet results are greatly at variance with the observations of the surface that allow an abrasion rate of approximately  $10^{-3}$  meters per million years (4). Thus either the observation is faulty, or the assumptions upon which the calculation is based must be in error to explain the large apparent discrepancy. We consider first that the impacting material may not be quartz (11); although any other "solid" material would also result in high abrasion rates. In many areas of Mars, the sediment supply may be limited, so that  $q$  is much smaller than wind tunnel tests at that wind speed would indicate. Perhaps the assumption having the greatest effect is the size of the impacting particle. Sagan et al. (12) suggested that sand sized material would quickly self destruct into micron-sized particles due to high energy saltation impacts. Observations of atmospheric dust (13,14) and spectral reflectance information (15) support the idea that there is a large amount of material in the martian surface environment on the order of a micron in diameter. It has been suggested by Greeley (16) that this fine sediment forms aggregates bound in part by electrostatic forces. These aggregates may be strong enough to saltate and form dunes and drifts, but would disintegrate upon impact rather than abrade surface rocks. The efficiency of abrading targets by such aggregates is currently under investigation.

In summary, sufficient laboratory work has been done on the martian abrasion problem to show that there is a major difference between the calculated rate of aeolian abrasion and the limits placed on that rate by the observation of surface features at the Viking landing sites. Further work is being done to investigate this discrepancy, but it is quite likely that it is due, at least in part, to the existence of aggregates of fine particles rather than sand size particles on the martian surface.

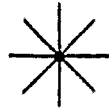
### REFERENCES

1. Greeley R. and Williams S. H. (1979) *Lunar & Planetary Sci.*, 10, 461-463 (abstract).
2. Krinsley D. et al. (1979) *Icarus*, 39, 364-384.
3. Sagan C. (1973) *JGR*, 78, 4155-4161.
4. Arvidson R. E. et al. (1979) *Nature*, 278, 533-535.
5. Moore H. J. et al. (1977) *JGR*, 82, 4497-4523.
6. Greeley R. and Williams S. H. (1979) *Rep. Planet. Geol. Program, TM-81776*, 241-243.
7. White, B. (1979) *JGR*, 84, 4643-4651.
8. Suzuki T. and Takahashi K., submitted to *J. Geol.*
9. Williams G. (1964) *Sediment.*, 3, 257-287.

**WIND EROSION ON MARS: RATE OF ABRASION ESTIMATE****Williams and Greeley**

10. Ryan J. A., personal communication, 11/79, 1/80.
11. Smalley I. and Kricsley D. (1979) submitted to *Icarus*.
12. Sagan C. et al. (1977) *JGR*, 82, 4430-4438.
13. Pollack J. B. et al. (1977) *JGR*, 82, 4479-4496.
14. Toon O. B. et al. (1977) *Icarus*, 30, 663-696.
15. Huck F. O. et al. (1977) *JGR*, 82, 4401-4411.
16. Greeley R. (1979) *JGR*, 84, 6248-6254.





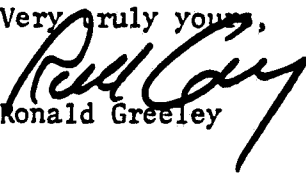
July 8, 1980

Mr. Angelo P. Margozzi  
Atmospheric Experiments Branch  
Mail Stop 245-5  
NASA Ames Research Center  
Moffett Field, CA 94035

Dear Angelo:

Transmitted herewith are three copies of the final report for NASA Ames Grant NSG-2286 entitled "Wind Tunnel Simulation of Martian Sand Storms."

Very truly yours,

  
Ronald Greeley

RG:pw

Enclosures

xc: Univeristy Affairs Office, NASA Ames  
Office of Grants & Contracts, SC  
NASA Scientific and Technical  
Information Facility (2 copies)